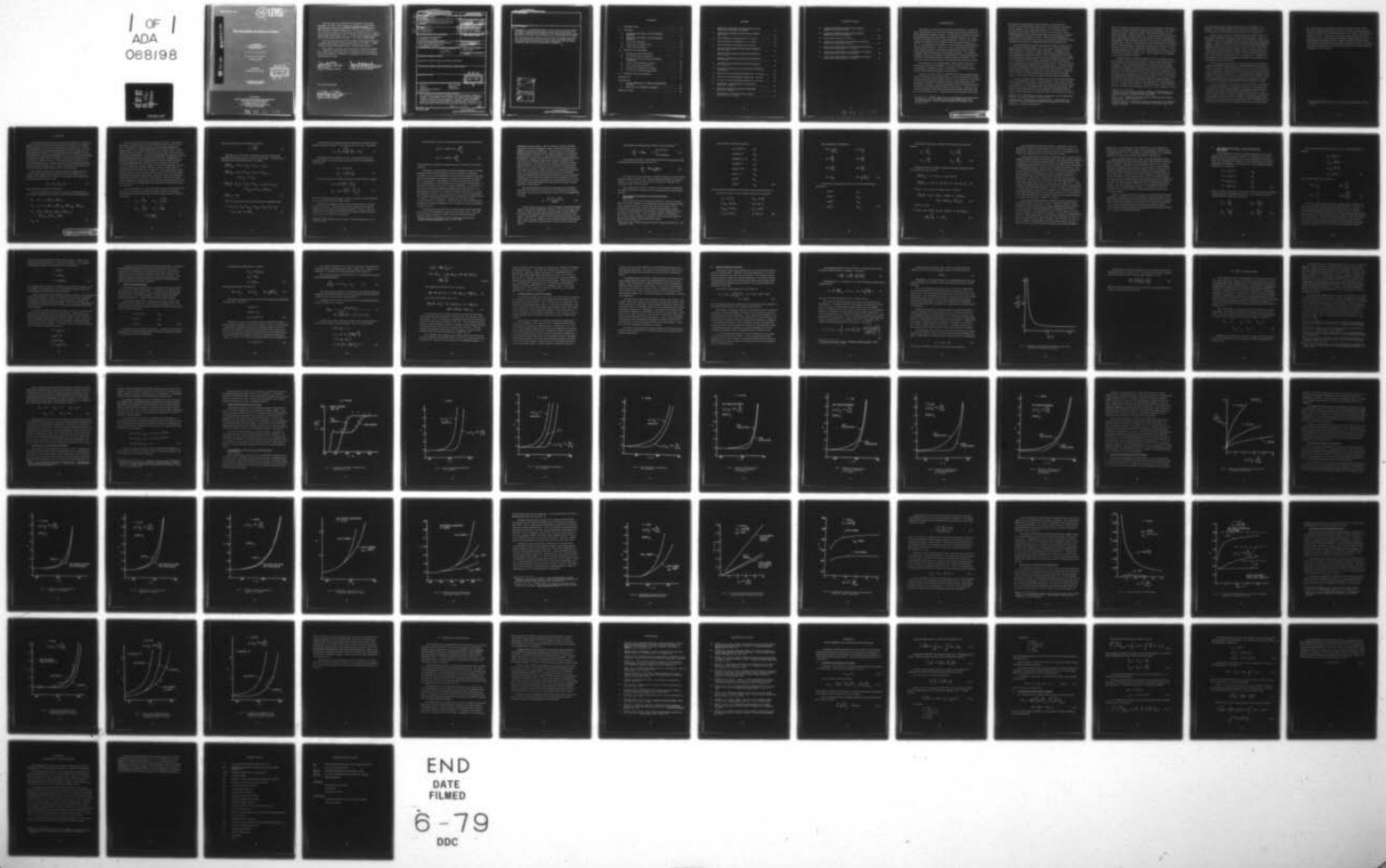
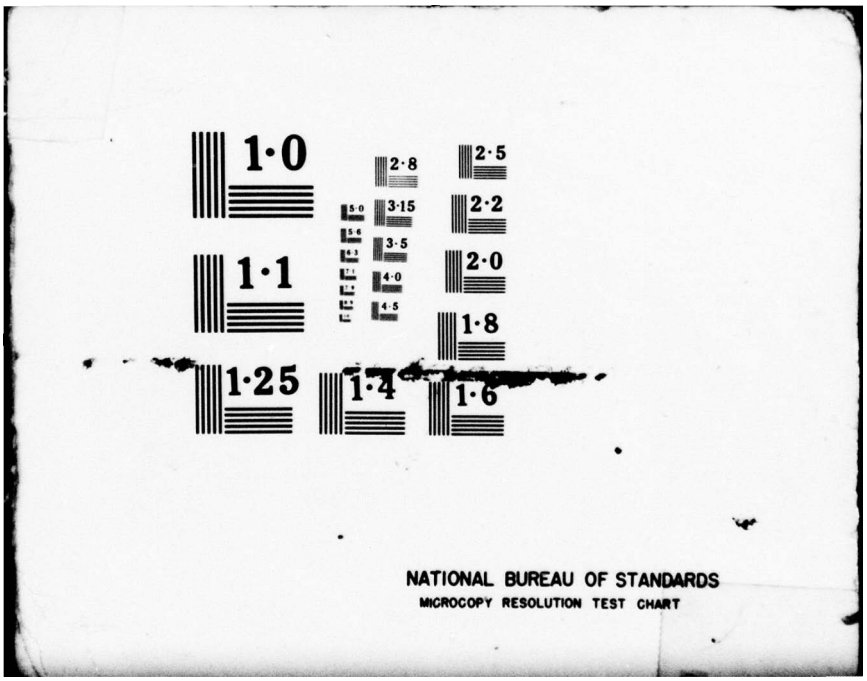
AD-A068 198 AEROSPACE CORP EL SEGUNDO CALIF VEHICLE ENGINEERING DIV F/G 21/2
THE NONEQUILIBRIUM ABLATION OF CARBON.(U)
NOV 78 P G CROWELL
UNCLASSIFIED TR-0079(4550-76)-1 SAMSO-TR-79-6 F04701-78-C-0079 NL

1 OF 1
ADA
068198



END
DATE
FILMED
6-79
DDC


1·0
1·1
1·25
2·8
3·15
3·5
4·0
4·5
1·4
2·5
2·2
2·0
1·8
1·6
NATIONAL BUREAU OF STANDARDS
MICROCOPY RESOLUTION TEST CHART

REPORT SAMSO-TR-79-6

(12) LEVEL II

DDC FILE COPY AD A068198

The Nonequilibrium Ablation of Carbon

P. G. CROWELL
Vehicle Engineering Division
Engineering Group

15 November 1978

Final Report
(September 1977-June 1978)

DDC
RECEIVED
MAY 3 1979
B

APPROVED FOR PUBLIC RELEASE;
DISTRIBUTION UNLIMITED

Prepared for

SPACE AND MISSILE SYSTEMS ORGANIZATION
AIR FORCE SYSTEMS COMMAND
Los Angeles Air Force Station
P.O. Box 92960, Worldway Postal Center
Los Angeles, Calif. 90009

79 05 02 010

This final report was submitted by The Aerospace Corporation, El Segundo, CA 90245, under Contract No. F04701-77-C-0078 with the Space and Missile Systems Organization, Deputy for Reentry Systems, P.O. Box 92960, Worldway Postal Center, Los Angeles, CA 90009. It was reviewed and approved for The Aerospace Corporation by E.G. Hertler, Vehicle Engineering Division, and R. E. Herold, Reentry Systems Division. The Air Force project officer was Capt. J. W. Bohlen, SAMSO/RSSE.

This report has been reviewed by the Office of Information (OI) and is releasable to the National Technical Information Service (NTIS). At NTIS it will be available to the general public, including foreign nations.

This technical report has been reviewed and is approved for publication. Publication of this report does not constitute Air Force approval of the report's findings or conclusions. It is published only for the exchange and stimulation of ideas.

James W. Bohlen

James W. Bohlen, Capt USAF
Project Officer
Reentry Technology Division

James M. McCormack

James M. McCormack, Lt Col, USAF
Chief, Reentry Technology Division
Deputy for Reentry Systems

FOR THE COMMANDER

William D. Goldberg

WILLIAM GOLDBERG, Colonel, USAF
Director, Systems Technology
Deputy for Reentry Systems

UNCLASSIFIED

SECURITY CLASSIFICATION OF THIS PAGE (When Data Entered)

REPORT DOCUMENTATION PAGE	READ INSTRUCTIONS BEFORE COMPLETING FORM
1. REPORT NUMBER: SAMSO-TR-79-6	2. GOVT ACCESSION NO. / 3. RECIPIENT'S CATALOG NUMBER
4. TITLE (and Subtitle): THE NONEQUILIBRIUM ABLATION OF CARBON.	5. TYPE OF REPORT & PERIOD COVERED: Final Report. Sept 77-Jun 78,
	6. PERFORMING ORG. REPORT NUMBER: TR-0079(4550-76)-1
7. AUTHOR(s): P.G. Crowell	8. CONTRACT OR GRANT NUMBER(s): F04701-78-C-0079 F04701-78-C-0078
9. PERFORMING ORGANIZATION NAME AND ADDRESS: The Aerospace Corporation, El Segundo, CA 90245	10. PROGRAM ELEMENT, PROJECT, TASK AREA & WORK UNIT NUMBERS
11. CONTROLLING OFFICE NAME AND ADDRESS: Space and Missile Systems Organization, Air Force Systems Command, Los Angeles, CA 90009	12. REPORT DATE: 15 Nov 78 / 13. NUMBER OF PAGES: 82
14. MONITORING AGENCY NAME & ADDRESS (if different from Controlling Office) 12 88p.	15. SECURITY CLASS. (of this report): Unclassified / 15a. DECLASSIFICATION/DOWNGRADING SCHEDULE

16. DISTRIBUTION STATEMENT (of this Report)

Approved for public release; distribution unlimited.

17. DISTRIBUTION STATEMENT (of the abstract entered in Block 20, if different from Report)

DDC RECEIVED MAY 3 1979 B

18. SUPPLEMENTARY NOTES

19. KEY WORDS (Continue on reverse side if necessary and identify by block number)

Carbon
Ablation
Nonequilibrium Ablation
Sublimation
Mass Transfer
Oxidation
Vaporization

20. ABSTRACT (Continue on reverse side if necessary and identify by block number)

A comprehensive analysis is presented of the nonequilibrium ablation of carbon in an atmosphere whose elemental composition consists of Oxygen, Nitrogen, Carbon and an inert species. The scope of the investigation ranges from the low surface temperature regime, where the ablation process is dominated by kinetically controlled oxidation reactions, to the high temperature sublimation regime dominated by rate-controlled →

409 369

DD FORM 1473 (FACSIMILE)

UNCLASSIFIED

SECURITY CLASSIFICATION OF THIS PAGE (When Data Entered)

19. KEY WORDS (Continued)

20. ABSTRACT (Continued)

vaporization. A detailed examination is made of the commonly employed assumption concerning the gas-phase and gas-solid reaction rates. In particular, calculations are presented for the limiting assumptions of fast (equilibrium) and slow (frozen) homogeneous and heterogeneous reactions.

The vaporization from a liquid carbon melt layer is analyzed and calculations are presented for the surface mass loss and melt layer thickness. Comparisons are made with the available experimental data and recommendations made for future experimental investigation.

ACCESSION for
NTIS White Section ✓
DDC Buff Section ☐
UNANNOUNCED ☐
JUSTIFICATION
BY
DISTRIBUTION/AVAILABILITY CODES
Dist. AVAIL. and/or SPECIAL
A

CONTENTS

I. INTRODUCTION 5

II. ANALYSIS 11

A. Equilibrium Gas Phase--Slow Nitridization Reactions 17

B. Equilibrium Gas Phase--Fast Nitridization Reactions 23

C. Frozen Carbon Species 26

D. Vaporization of Molten Carbon 30

E. Surface Energy Balance 32

III. RESULTS AND DISCUSSION 37

A. Kinetically Controlled Oxidation 39

B. Slow Nitridization Calculations 41

C. Comparison of Fast and Slow Nitridization Assumptions 41

D. Frozen Carbon Sublimation Species 50

E. Carbon Melt Layer Calculations 52

F. Steady-State Conduction Assumption 63

G. Comparison with Experimental Data 66

IV. SUMMARY AND CONCLUSIONS 71

REFERENCES 73

APPENDICES:

A. VAPOR PRESSURE OF CARBON SUBLIMATION SPECIES 75

B. SELECTION OF CHEMICAL SPECIES 81

NOMENCLATURE 83

FIGURES

1. Influence of Time Scale and Recession Rate on the Steady-State Conduction Assumption 35

2. Comparison with Exact Calculations for Oxidation Mass Loss 42

3. Slow Nitridization Calculations (P = 0.10 atm) 43

4. Slow Nitridization Calculations (P = 1.0 atm) 44

5. Slow Nitridization Calculations (P = 100 atm) 45

6. Influence of Heterogeneous Nitridization Reactions (P = 0.10 atm) 46

7. Influence of Heterogeneous Nitridization Reactions (P = 1.0 atm) 47

8. Influence of Heterogeneous Nitridization Reactions (P = 1.0 atm) 48

9. Influence of Heterogeneous Nitridization Reactions (P = 100 atm) 49

10. Maximum B' Difference for Fast and Slow Nitridization Assumptions 51

11. Influence of Frozen Sublimation Species (P = 0.10 atm) 53

12. Influence of Frozen Sublimation Species (P = 1.0 atm) 54

13. Influence of Frozen Sublimation Species (P = 100 atm) 55

14. Equilibrium Vaporization from a Carbon Melt Layer (P = 1.0 atm) 56

15. Equilibrium Vaporization from a Carbon Melt Layer (P = 100 atm) 57

16. Nonequilibrium Vaporization from a Carbon Melt Layer (P = 1.0 atm) 59

FIGURES (Continued)

17. Comparison of Solid and Liquid Carbon Ablation Models for Surface Recession 60

18. Comparison of Solid and Liquid Carbon Ablation Models for Surface Temperature 61

19. Steady-State Melt Layer Thickness 64

20. Comparison of Steady-State and Transient Conduction Models for Surface Mass Transfer 65

21. Comparison of Equilibrium and Nonequilibrium Ablation Models with Lundell Data (P = 1.0 atm) 67

22. Comparison of Equilibrium and Nonequilibrium Ablation Models with Maurer Data (P = 0.86 atm) 68

23. Comparison of Equilibrium and Nonequilibrium Ablation Models with Maurer Data (P = 0.22 atm) 69

79 05 02 010

I. INTRODUCTION

The ablation of carbon may be classified as equilibrium or nonequilibrium, depending upon the nature of the heterogeneous surface reactions and the homogeneous gas-phase reactions. If the gas-phase reactions, as well as the heterogeneous carbon vaporization and oxidation reactions, are in equilibrium, the ablation process is termed equilibrium, and the mass transfer coefficient is obtained from the diffusion-controlled approximation (e.g., Ref. 1). The equilibrium assumption is easily utilized and sufficiently accurate for many applications. There are, however, situations wherein the carbon ablation process is dominated by nonequilibrium effects, such as kinetically controlled oxidation and sublimation reactions. Also included among the nonequilibrium effects is the possibility of frozen gas phase reactions and/or frozen heterogeneous reactions with the solid carbon. This report is concerned with the realm of the nonequilibrium ablation of carbon.

The available work on nonequilibrium carbon ablation suffers from several major and minor limitations. First, the scope of the previous investigations is generally limited to the oxidation or sublimation regime instead of both regions being treated simultaneously.

A second, and more serious, criticism concerns the postulated model for the gas-phase and gas-solid reactions. Due to a complete lack of kinetics data for most of the reaction rates of interest, it is necessary to invoke either the frozen or equilibrium assumption for many of the heterogeneous and homogeneous reactions. Various combinations of the frozen and equilibrium assumptions have been utilized to obtain the ablation rate. However, there exists no systematic examination of the influence of these assumptions upon the calculated ablation rates. Apparently the only investigation concerning

---

[1] Crowell, P.G., "Analytic Solutions for Carbon Sublimation in Atmospheres of Elemental Carbon, Hydrogen, Nitrogen and Oxygen," Report No. TR-0078(3550-15)-2, The Aerospace Corporation, El Segundo, Calif., December 1977.

PRECEDING PAGE BLANK-NOT FILMED

the influence of the postulated chemistry model is a limited study by Maurer[2] to examine the effect of the frozen versus equilibrium assumption for the gas-phase carbon sublimation species. The sensitivity studies contained in the literature deal with the influence of the allowed species, the thermochemical data used for each species, the vaporization coefficients for the sublimation reactions, et cetera. While such investigations are necessary, it is felt that the basic choice of a model for the reactions (frozen/equilibrium) may also exert significant influence on the ablation rate.

A third consideration concerns the possible melting of carbon and its impact upon the predicted ablation rate. The only work on the influence of carbon melting is an equilibrium study by Kratsch[3]. Although the exact melt temperature is not known, several experimental investigations yield values ranging from 3800°K to 4300°K. Surface temperatures in this range are often predicted utilizing models which assume ablation from solid carbon only. Furthermore, there have been suggestions* that the "mechanical" erosion observed in some ground tests is actually due to molten carbon being stripped off the ablating specimen by aerodynamic forces. If molten carbon does form, the ablation rate will be different than that obtained from a solid carbon surface due either to mechanical removal of the melt or a difference in vapor pressures in going from the gas-solid system to the gas-liquid system. In any event, this is an area that warrants further investigation.

The fourth critique of the available work involves the solution procedure used to obtain numerical results. In many instances, the numerical method is not described. In those cases in which it is described, the method involves a cumbersome, time-consuming scheme with multiple iteration loops. Most of the difficulty experienced by some investigators in obtaining numerical results is due to their choice of chemistry model for the gas-phase reactions.

---

[2] Maurer, R.E., "An Evaluation of Some Uncertainties in Carbon Sublimation Kinetics," Aerotherm TM-73-27, January 1973.

[3] Kratsch, K.M., "Graphite Fusion and Vaporization," ASME/AIAA 10th Structures, Structural Dynamics and Materials Conference, April 1969.

* Baker, R. L., Private communication

That is, the impact of the gas-phase frozen versus equilibrium assumption on the numerical solution technique is apparently not recognized. Thus, while Dolton[4] and Baker[5] required a multiple, nested iteration scheme for the frozen assumption, Ziering[6] needed only a single iteration for the equilibrium case. The solution procedure is not important if the intent is to generate a set of tables of mass transfer parameter (B') for input into a thermodynamic response code. However, since the mass transfer parameter is a function of three variables (pressure, temperature, and heat flux), this approach would require a very tedious three-dimensional interpolation procedure. A more desirable approach is the utilization of a surface chemistry subroutine called from the thermodynamic response code. In this situation, the computation speed obviously becomes critical.

Whether the minor limitations alluded to earlier are indeed minor or major depends on the particular situation. A case in point involves the solution of the surface energy balance and the utilization of the steady-state assumption. If the surface temperature is a specified boundary condition, then the energy balance is not solved and the steady-state assumption is not required. If, on the other hand, the temperature must be obtained as part of the solution, the energy balance is required, and the heat flux conducted into the ablating surface must be modeled in some manner. In order to uncouple the solution of the surface energy balance from the in-depth conduction problem, the steady-state assumption is frequently used to approximate the heat flux conducted into the interior. This assumption is usually justified on the basis of simplicity and reasonable accuracy. In many situations, however,

---

[4] Dolton, T.A., R.E. Maurer, and H.E. Goldstein, "Thermodynamic Performance of Carbon in Hyperthermal Environments," AIAA 3rd Thermophysics Conference, Paper No. 68-754, June 1968.

[5] Baker, R.L., "Graphite Sublimation Chemistry Nonequilibrium Effects," AIAA Journal, 15(10), October 1977.

[6] Ziering, M.B. and V. DiCristina, "Thermomechanical Erosion of Ablative Plastic Composites," AIAA 7th Thermophysics Conference, April 1972, Paper No. 72-299.

the requirements for the validity of the steady-state assumptions (i.e., large time and small thermal penetration depth) are not satisfied, and its use will result in a considerable overprediction of the recession rate.

Another "minor" criticism of the nonequilibrium ablation studies concerns the inconsistencies present in many of the formulations. These inconsistencies arise as a consequence of the choice of chemical reaction rate model (i.e., frozen or equilibrium) used for the gas-phase and heterogeneous reactions. That is, the use of a mixed set of rate-controlled and diffusion-controlled heterogeneous surface reactions leads to arbitrary restrictions being imposed on the allowable gas-phase reactions in order that the rate-controlled reactions not be short-circuited. Similar difficulties arise when the carbon sublimation species are frozen in the gas phase. Whether the inconsistencies are numerically significant depends on the particular set of assumptions and allowable species.

It is the purpose of this report to critically examine each of the above deficiencies in the existing formulations for the nonequilibrium ablation of carbon. In particular, detailed computations will be carried out to examine various assumptions concerning the chemical model, and comparisons will be made with the existing ablation data. A computationally fast solution scheme, suitable for subroutine use, will be developed for the recommended formulation. Recommendations for future development and testing will be made to address those uncertainties that impact the predicted ablation of carbon.

Before proceeding to the formulation of the next section, some ground rules should be established. The interest of this report is the ablation of carbon in an atmosphere whose elemental composition consists of carbon, nitrogen, oxygen, and an inert element (denoted by the symbol I). This system clearly includes air (oxygen, nitrogen, and argon) as a special case. If the gas phase is assumed to be in equilibrium, the boundary layer edge elemental mass fractions will be presumed to be known. Furthermore, the edge species mass fraction will be assumed known for any frozen species.

The surface pressure, temperature, and convective heat transfer (either blowing or nonblowing) are considered known. Only the dominant gas-phase species (as determined from previous analyses) for a system of this elemental composition will be considered as well as the first five carbon sublimation species ($C_1 \rightarrow C_5$). Unless otherwise indicated, JANNAF[7] values will be used for all species thermochemical data. Since it is intended that this formulation be used in conjunction with a simplified boundary layer analysis, the usual simplifying assumptions (unity Lewis and Prandtl numbers and equal diffusion coefficients) will be invoked.

[7] JANNAF Thermochemical Tables, National Bureau of Standards, NBS-37, June 1971.

II. ANALYSIS

As indicated above, the major objective of this report is to examine the influence of the assumed chemical state upon the predicted mass transfer. This examination is carried out in Subsections II-A through II-D. The first two subsections assume gas-phase equilibrium with frozen (Subsection II-A) and equilibrium (Subsection II-B) heterogeneous carbon-nitrogen reactions. In Subsection II-C, the carbon sublimation species are frozen in the gas phase. The analyses of Subsections II-A through II-C ignore the possibility of the formation of a carbon melt layer. The carbon melt layer problem is considered in Subsection II-D. Finally, the validity of the steady-state assumption is examined in Subsection II-E. Much of the analysis is independent of the assumed chemical state; this analysis is considered next.

The problem of interest is to calculate the mass transfer from an ablating carbon surface (solid or liquid) over which a boundary layer is flowing. The elemental mass fractions at the boundary layer edge are presumed known and must sum to unity.

$$\tilde{K}_{N_e} + \tilde{K}_{O_e} + \tilde{K}_{C_e} + \tilde{K}_{I_e} = 1 \tag{1}$$

where subscript I denotes the inert species.

At the wall (solid-gas or liquid-gas interface), the elemental mass fractions are specified in terms of the species of interest (see Appendix B).

$$\tilde{K}_{O_w} = K_O + K_{O_2} + \frac{16}{28} K_{CO} + \frac{32}{44} K_{CO_2}$$

$$\tilde{K}_{N_w} = K_N + K_{N_2} + \frac{14}{26} K_{CN} + \frac{28}{52} K_{C_2N_2} + \frac{28}{76} K_{C_4N_2} + \frac{14}{38} K_{C_2N}$$

$$\tilde{K}_{C_w} = \frac{12}{28} K_{CO} + \frac{12}{44} K_{CO_2} + \frac{12}{26} K_{CN} + \frac{24}{52} K_{C_2N_2} + \\ + \frac{48}{76} K_{C_4N_2} + \frac{24}{38} K_{C_2N} + \sum K_{C_i}$$

$$\tilde{K}_{I_w} = K_I \tag{2}$$

PRECEDING PAGE BLANK-NOT FILMED

Some comments about the chosen species are in order. The temperature range of interest extends from 540 to 9000°R and the pressure range from 0.10→300 atm. All these species are numerically significant in various portions of the indicated temperature and pressure ranges. Since a unified treatment is sought over the entire range, all these species must be considered simultaneously. As will be demonstrated later, this set of species does not pose any particular computational difficulties. Although atomic oxygen and nitrogen are not dominant species, they may influence the ablation rate through kinetically controlled surface reactions and should be carried for generality. An inert species is included for generality, since it is present in many atmospheres of interest. The inert species does not react chemically, since the surface temperature is not high enough to cause significant ionization, but its presence does influence the molecular weight. Although the formulation contains only a single inert species, the analysis is easily generalized for any number of inert species. This may be done by simply redefining the ratio $\tilde{K}_I / M_I$ as the summation of this quantity over all the inert species and equating $\tilde{K}_I$ to the summation of all the inert elemental mass fractions.

The wall elemental mass fractions may be related to the boundary layer edge values by invoking the equivalence between mass and heat transfer (assuming equal diffusion coefficients and unity Prandtl and Lewis numbers). This yields

$$\tilde{K}_{O_w} = \frac{\tilde{K}_{O_e}}{1 + B'} \qquad \tilde{K}_{C_w} = \frac{B' + \tilde{K}_{C_e}}{1 + B'}$$

$$\tilde{K}_{N_w} = \frac{\tilde{K}_{N_e}}{1 + B'} \qquad \tilde{K}_{I_w} = \frac{\tilde{K}_{I_e}}{1 + B'}$$

$$B' \equiv \frac{\dot{m}}{\rho_e u_e C_H} \tag{3}$$

The partial pressure of any constituent is given as

$$P_i = \frac{PMK_i}{M_i} \tag{4}$$

Equation (2) is cast in terms of partial pressures by multiplying through by the product of pressure and molecular weight. This operation, in conjunction with the substitution of Eq. (3), yields

$$\frac{PM}{1+B'}\tilde{K}_{O_e} = 16\,P_O + 32\,P_{O_2} + 16\,P_{CO} + 32\,P_{CO_2}$$

$$\frac{PM}{1+B'}\tilde{K}_{N_e} = 14\,P_N + 28\,P_{N_2} + 14\,P_{CN} + 28\,P_{C_2N_2} + 28\,P_{C_4N_2} + 14\,P_{C_2N}$$

$$\frac{PM}{1+B'}\left(B' + \tilde{K}_{C_e}\right) = 12\,P_{CO} + 12\,P_{CO_2} + 12\,P_{CN} + 24\,P_{C_2N_2} + 48\,P_{C_4N_2} + 24\,P_{C_2N} + \sum M_{C_i} P_{C_i}$$

$$\frac{PM}{1+B'}\tilde{K}_{I_e} = M_I P_I \tag{5}$$

The sum of the partial pressures must equal the mixture pressure.

$$P = P_N + P_{N_2} + P_{CN} + P_{C_2N_2} + P_{C_4N_2} + P_{C_2N} + P_O + P_{O_2} + P_{CO} + P_{CO_2} + P_I + \sum P_{C_i} \tag{6}$$

The kinetically controlled vaporization reactions are modeled with the Knudsen-Langmuir equation.[8] This yields the mass loss due to sublimation

$$\dot{m}_{C_i} = \beta_{C_i} \sqrt{\frac{M_{C_i}}{2\pi RT}} \left(P^v_{C_i} - P_{C_i} \right) \tag{7}$$

The heterogeneous oxidation reactions, involving both atomic and molecular oxygen, are also kinetically controlled and are represented by the following:

$$\dot{m}_O = F_O \left(T, P_O \right)$$

$$\dot{m}_{O_2} = F_{O_2} \left(T, P_{O_2} \right) \tag{8}$$

In many instances, the oxidation reactions are represented as follows:

$$F_O = K_O(T) \left(P_O^{n_O} - P_{O_{eq}}^{n_O} \right)$$

$$F_{O_2} = K_{O_2}(T) \left(P_{O_2}^{n_{O_2}} - P_{O_{2_{eq}}}^{n_{O_2}} \right) \tag{9}$$

where the coefficients K_O and K_{O_2} are Arhenius functions, and the exponents n_O and n_{O_2} indicate the order of the reaction.

Note that the equilibrium values of the partial pressures are usually deleted from Eq. (9). This is because they are usually several orders of magnitude smaller than the actual partial pressures. They are, however, included here to provide a formal means of zeroing the oxidation mass loss as heterogeneous equilibrium is approached.

---

[8] Kennard, E.H., "Kinetic Theory of Gases," McGraw-Hill Book Co., Inc., New York, 1938.

The equilibrium values for the partial pressures may be obtained from

$$K_P\ (2C^* + O_2 \rightleftarrows 2\ CO) = \frac{P_{CO}^2}{P_{O_{2_{eq}}}}$$

$$K_P\ (C^* + O \rightleftarrows CO) = \frac{P_{CO}}{P_{O_{eq}}} \qquad (10)$$

where the pressure equilibrium constants (K_P) are defined for the indicated reactions.

In principle, the heterogeneous carbon nitridization reactions involving both atomic and molecular nitrogen could also be treated as kinetically controlled. That is, the nitridization mass loss could be modeled in the same manner as the oxidation through the use of expressions analogous to those of Eqs. (8) through (10). Unfortunately, the almost complete lack of kinetics data on heterogeneous carbon-nitrogen reactions precludes this approach. In the absence of reaction rate data for carbon nitridization, recourse must be made to the limiting assumptions of infinitely fast surface reactions (i.e., heterogeneous equilibrium) or infinitely slow surface reactions (i.e., frozen heterogeneous reactions). It is this choice of fast or slow surface nitridization reactions which characterizes the earlier nonequilibrium ablation studies. For example, Dolton[4] and Maurer[2] assumes fast reactions, whereas Ziering[6] assumes slow reactions. As indicated above, the slow nitridization assumption is examined in Subsection II-A, and the fast reaction assumption in Subsection II-B.

A literature search yielded only one reference (9) on the experimental determination of heterogeneous carbon-nitrogen reaction rates. This data has been analyzed to determine which of the two limiting nitridization

[9]Goldstein, H. W., "The Reaction of Active Nitrogen with Graphite," Journal of Physical Chemistry, 68(1), January 1964.

assumptions is most realistic. The test consisted of heating a graphite specimen to 2365°K and impinging a stream of molecular nitrogen onto its surface at a pressure of 0.00256 atm. The test was run for 30 minutes, and the gas phase was condensed out in liquid-nitrogen traps and examined for the presence of cyanogen. A mass transfer prediction, assuming fast heterogeneous reactions, indicated that the amount of cyanogen produced was several orders of magnitude larger than the detection threshold of the experimental setup. The calculation was repeated, assuming slow heterogeneous reactions, and yielded an amount of cyanogen about equal to the detection limit. Since no cyanogen was detected, it is concluded that the nitridization reactions are closer to the frozen limit than to the equilibrium limit. Due to uncertainties about the experiment and the assumptions required to analyze the data (particularly the estimate for the mass transfer coefficient), this conclusion can hardly be viewed as definitive. However, in the absence of any other information, this result indicates that it is more reasonable to ignore heterogeneous nitridization reactions than to assume that they are in equilibrium.

Since the nitridization reactions are not assumed to be kinetically controlled, the total mass loss is the sum of the sublimation and oxidation components. The mass loss is expressed in terms of B' by dividing through by $\rho_e u_e C_H$.

$$B' = \frac{\dot{m}_O + \dot{m}_{O_2} + \sum \dot{m}_{C_i}}{\rho_e u_e C_H} \qquad (11)$$

The heat transfer ($\rho_e u_e C_H$) is obviously dependent upon the fluid dynamic aspects of the particular application of interest. Since it is the intent of this report to uncouple the surface mass transfer problem from the solution of the boundary layer equations, the heat transfer must be modeled in some manner. One approach is simply to solve the mass transfer problem for specified values of $\rho_e u_e C_H$. However, since it is itself a function of the blowing rate, it is more useful to obtain solutions in terms of the nonblowing heat transfer.

The blowing and nonblowing heat transfer will be related by[10]

$$\frac{C_H}{C_{H_0}} = \frac{1}{1 + \eta B'} \qquad \eta = \begin{cases} 0.60 \text{ laminar} \\ \\ 0.30 \text{ turbulent} \end{cases} \tag{12}$$

In a number of instances, experimental data has been interpreted using the following result for laminar flow (ref. 22)

$$\frac{C_H}{C_{H_0}} = \frac{\ell n(1 + 1.28\, B')}{1.28\, B'} \tag{13}$$

For values of B' up to about three, both these expressions yield virtually identical results for laminar flow. When analyzing data which was reduced with Eq. (13), this report will use the same expression. Otherwise, the expression of Eq. (12) will be used.

This completes the analysis common to all the subsections that follow. The specific reactions are peculiar to each subsection and are considered as required.

A. EQUILIBRIUM GAS PHASE--SLOW NITRIDIZATION REACTIONS

In this section, the mass transfer formulation is closed by assuming that all gas-phase reactions are in equilibrium and that heterogeneous nitridization reactions take place so slowly that they may be ignored. Thus, carbon-nitrogen species are formed solely through gas-phase reactions. Ziering[6] was apparently the first investigator to model nonequilibrium carbon ablation in this manner. This formulation differs from Ziering's in that a larger number of species is considered, and the oxidation regime is treated simultaneously with the sublimation regime.

[10] Dorrance, W.H., "Viscous Hypersonic Flow," McGraw-Hill Book Co., Inc., New York, 1962.

The gas-phase reactions are given by

$$
\begin{aligned}
N_2 + 2C &\rightleftarrows 2\,CN && K_{P_1} \\
C_2N_2 &\rightleftarrows 2\,CN && K_{P_2} \\
C_4N_2 &\rightleftarrows 2\,CN + 2C && K_{P_3} \\
C_2N &\rightleftarrows CN + C && K_{P_4} \\
CO_2 &\rightleftarrows C + 2O && K_{P_5} \\
CO &\rightleftarrows C + O && K_{P_6} \\
O_2 &\rightleftarrows 2O && K_{P_7} \\
N_2 &\rightleftarrows 2N && K_{P_8}
\end{aligned}
\qquad (14)
$$

where the pressure equilibrium constants are for the indicated reactions.

The partial pressures for the indicated reactions are related by

$$
\begin{aligned}
P_{N_2} &= \alpha_1 P_{CN}^2 & P_{CO_2} &= \alpha_5 P_O^2 \\
P_{C_2N_2} &= \alpha_2 P_{CN}^2 & P_{CO} &= \alpha_6 P_O \\
P_{C_4N_2} &= \alpha_3 P_{CN}^2 & P_{O_2} &= \alpha_7 P_O^2 \\
P_{C_2N} &= \alpha_4 P_{CN} & P_N &= \alpha_8 P_{CN}
\end{aligned}
\qquad (15)
$$

The α coefficients are defined by

$$\alpha_1 \equiv \frac{1}{P_C^2 K_{P_1}} \qquad \alpha_2 \equiv \frac{1}{K_{P_2}}$$

$$\alpha_3 \equiv \frac{P_C^2}{K_{P_3}} \qquad \alpha_4 \equiv \frac{P_C}{K_{P_4}}$$

$$\alpha_5 \equiv \frac{P_C}{K_{P_5}} \qquad \alpha_6 \equiv \frac{P_C}{K_{P_6}}$$

$$\alpha_7 \equiv \frac{1}{K_{P_7}} \qquad \alpha_8 \equiv \sqrt{\alpha_1 K_{P_8}} \tag{16}$$

The gas-phase dissociation reactions for the carbon sublimation species are

$$C_2 \rightleftarrows 2C \qquad K_{P_9}$$

$$C_3 \rightleftarrows 3C \qquad K_{P_{10}}$$

$$C_4 \rightleftarrows 4C \qquad K_{P_{11}}$$

$$C_5 \rightleftarrows 5C \qquad K_{P_{12}} \tag{17}$$

The pressure equilibrium constants relate the partial pressures as follows:

$$K_{P_9} = \frac{P_C^2}{P_{C_2}} \qquad K_{P_{10}} = \frac{P_C^3}{P_{C_3}}$$

$$K_{P_{11}} = \frac{P_C^4}{P_{C_4}} \qquad K_{P_{12}} = \frac{P_C^5}{P_{C_5}} \tag{18}$$

Substitution of Eq. (15) into the oxygen and nitrogen elemental conservation equations of Eq. (5) yields

$$\frac{PM}{1+B'}\tilde{K}_{O_e} = 16\,(1+\alpha_6)\,P_O + 32\,(\alpha_5+\alpha_7)\,P_O^2$$

$$\frac{PM}{1+B'}\tilde{K}_{N_e} = 28\,(\alpha_1+\alpha_2+\alpha_3)\,P_{CN}^2 + 14\,(1+\alpha_4+\alpha_8)\,P_{CN} \tag{19}$$

Similarly, the carbon mass balance of Eq. (5) becomes

$$\frac{PM}{1+B'}\left(B' + \tilde{K}_{C_e}\right) = 12\alpha_6 P_O + 12\alpha_5 P_O^2 + (12+24\alpha_4)P_{CN} + \\ + (24\alpha_2 + 48\alpha_3)P_{CN}^2 + \sum M_{C_i} P_{C_i} \tag{20}$$

Equation (6) yields

$$(1+\alpha_6)P_O + (\alpha_5+\alpha_7)P_O^2 + (\alpha_1+\alpha_2+\alpha_3)P_{CN}^2 + (1+\alpha_4+\alpha_8)P_{CN} + \\ + \frac{PM}{1+B'}\,\frac{\tilde{K}_{I_e}}{M_I} = P - \sum P_{C_i} \tag{21}$$

This completes the problem formulation. Specifically, the set of equations to be solved consists of Eqs. (11), (12) [or (13)], and Eqs. (18) through (21). Since one of the objectives is to examine computational efficiency, the solution procedure is now considered in detail.

A brief examination of the system of equations makes it obvious that an iterative solution procedure must be employed. Since the pressure equilibrium constants are known functions of temperature, it is apparent [see Eq. (18)] that guessing a partial pressure for any one of the carbon species immediately yields the partial pressure values for the remaining carbon species. Since C_3 is usually the dominant carbon species, we adopt Ziering's approach and iterate on the partial pressure of C_3. Thus, for a guessed value of P_{C_3}, the remaining P_{C_i} are evaluated from Eq. (18) and the α coefficients from Eq. (16). Next, Eqs. (19) and (21) are solved for P_O, P_{CN}, and $PM/(1+B')$. Then Eq. (20) is solved for B', the blowing heat transfer is evaluated from Eq. (12) [or (13)], and Eq. (11) is also solved for B'. If the values of B' obtained from Eqs. (11) and (20) agree to within some prescribed tolerance, the iteration has converged. If not, a new guess is made for the C_3 partial pressure, and the process repeated until convergence is achieved. The Newton-Raphson iteration is used, and the value of P_{C_3} is constrained to be less than the upper-bound value which is the equilibrium vapor pressure of C_3 or the mixture pressure, whichever is smaller.

The only computational problem encountered during the iteration is the solution of Eqs. (19) and (21). That is, these three equations may be combined to yield a quartic for P_O or P_{CN}. Although an analytic solution exists for a quartic, it was determined to be computationally faster to solve it iteratively. This iteration proceeds as follows: guess a value for P_O and solve Eq. (19) for $PM/(1+B')$ and P_{CN}. The guess is checked against Eq. (21). If the left-hand side is greater than the right-hand side (which is known), the guessed value of P_O is too large. If it is smaller, the value of P_O is too small. This procedure continuously defines upper- and lower-bound values for P_O which are used to constrain the next Newton-Raphson

guess for P_O. An initial upper-bound value for P_O is easily obtained by zeroing the CN partial pressure in Eq. (21) and combining it with the oxygen mass balance of Eq. (19). The solution is iterated until Eq. (21) is satisfied. Generally, this iteration converges within three or four guesses.

A few closing comments are in order. The only significant computational difference between this work and Ziering's is the necessity of solving a quartic, instead of a quadratic, inside the iteration loop for P_{C_3}. This is due to the inclusion of O_2 and CO_2 in the allowed species. If only the high-temperature sublimation regime were of interest, these two would be trace species and thereby deleted from the formulation by zeroing α_5 and α_7. In this manner, Eqs. (19) and (21) would yield a quadratic in P_{CN} instead of a quartic. Similarly, the computational effort could be reduced by splitting the sublimation and oxidation regimes into separate high- and low-temperature domains, solving each domain separately, and then patching them together. However, one of the objectives of this report is to develop a single unified analysis valid for any temperature regime. It is felt that the increased generality is well worth the slight computational penalty associated with solving the quartic.

Section I indicated that various approaches employing mixed frozen and equilibrium assumptions result in inconsistencies in the formulation. Note that no such inconsistencies are present in the formulation of this subsection. That is, the frozen nitridization assumption does not require the imposition of any artificial constraints upon the equilibrium gas-phase reactions. This is not the situation with respect to the equilibrium nitridization assumption, as will be seen in Subsection II-B.

B. EQUILIBRIUM GAS PHASE--FAST NITRIDIZATION REACTIONS

In this subsection, the alternate limiting assumption for the heterogeneous nitridization reactions is examined. In Subsection II-A, these reactions were assumed to take place so slowly that they could be ignored. Here, it is assumed that the reaction rates are sufficiently fast to insure heterogeneous equilibrium. Specifically, it is assumed that the following reactions are in equilibrium:

$$
\begin{aligned}
2C^{*} + N_2 &\rightleftarrows 2\,CN & K^{*}_{P_1} \\
2C^{*} + N_2 &\rightleftarrows C_2N_2 & K^{*}_{P_2} \\
4C^{*} + N_2 &\rightleftarrows C_4N_2 & K^{*}_{P_3} \\
4C^{*} + N_2 &\rightleftarrows 2\,C_2N & K^{*}_{P_4}
\end{aligned}
\qquad (22)
$$

where C^{*} denotes solid carbon, and the superscript asterisk on the equilibrium constants indicates a heterogeneous reaction. The partial pressures are related through the equilibrium constants by

$$
K^{*}_{P_1} = \frac{P^2_{CN}}{P_{N_2}} \qquad K^{*}_{P_2} = \frac{P_{C_2N_2}}{P_{N_2}}
$$

$$
K^{*}_{P_3} = \frac{P_{C_4N_2}}{P_{N_2}} \qquad K^{*}_{P_4} = \frac{P^2_{C_2N}}{P_{N_2}} \qquad (23)
$$

By rearrangment of these expressions, the following relationships are obtained:

$$P_{N_2} = \alpha_1^* P_{CN}^2$$

$$P_{C_2N_2} = \alpha_2^* P_{CN}^2$$

$$P_{C_4N_2} = \alpha_3^* P_{CN}^2$$

$$P_{C_2N} = \alpha_4^* P_{CN} \qquad (24)$$

where the α^* coefficients are defined by

$$\alpha_1^* \equiv \frac{1}{K_{P_1}^*} \qquad \alpha_2^* \equiv \frac{K_{P_2}^*}{K_{P_1}^*}$$

$$\alpha_3^* \equiv \frac{K_{P_3}^*}{K_{P_1}^*} \qquad \alpha_4^* \equiv \sqrt{\frac{K_{P_4}^*}{K_{P_1}^*}} \qquad (25)$$

With the exception of the homogeneous carbon-nitrogen reactions, the gas-phase reactions are identical to those of Subsection II-A. However, the first four reactions of Eq. (14) must be deleted in order to avoid short-circuiting the nonequilibrium sublimation reactions. That is, inclusion of these homogeneous carbon-nitrogen reactions, together with the heterogeneous reactions of Eq. (22), would force the partial pressure of each carbon sublimation species to be equal to its corresponding vapor pressure, thereby zeroing the Knudsen-Langmuir equations and imposing equilibrium upon the sublimation reactions. In order to prevent this, all gas-phase reactions

involving the carbon sublimation species and nitrogen or carbon-nitrogen species must be suppressed (i.e., assumed to be frozen). For example, the following reactions are not allowed to be in equilibrium:

$$C + N \rightleftarrows CN$$

$$C + CN \rightleftarrows C_2N$$

$$C_2 + N_2 \rightleftarrows C_2N_2 \qquad (26)$$

The only gas-phase reactions involving the carbon sublimation species which are allowed to be in equilibrium are the dissociation reactions of Eq. (17) and reactions involving carbon-oxygen compounds.

These restrictions on the allowable gas-phase reactions are accomplished simply by replacing the first four homogeneous reactions of Eq. (14) by the heterogeneous reactions of Eq. (22). This results in the coefficients α_1 through α_4 being replaced by α_1^* through α_4^*. This is the only change required in the analysis of Subsection II-A to implement the assumption of fast nitridization reactions.

It should be pointed out that the use of Eqs. (22) does not imply that the carbon-nitrogen species are frozen in the gas phase. While they are prohibited from reacting with the carbon sublimation species, they are allowed to be in equilibrium with nitrogen and with one another. That is, Eqs. (22) are exactly equivalent to any one of the heterogeneous reactions plus three equilibrium gas-phase reactions. For example, Eqs. (22) could be replaced by the following set of equivalent reactions:

$$2C^* + N_2 \rightleftarrows 2\ CN$$

$$C_2N_2 \rightleftarrows 2\ CN$$

$$C_4N_2 \rightleftarrows 2\ C_2N$$

$$N_2 + C_4N_2 \rightleftarrows 4\ CN \qquad (27)$$

In summary, the use of the fast nitridization assumption, in conjunction with nonequilibrium sublimation reactions, precludes the use of a self-consistent set of equilibrium reactions for the gas phase. Therefore, the validity of the fast nitridization assumption rests on the existence of an arbitrary mixed set of frozen and equilibrium gas-phase reactions. This seems somewhat implausible and must be regarded as casting additional doubt upon the fast nitridization assumption.

C. FROZEN CARBON SPECIES

In this subsection we examine the assumption that the carbon sublimation species are frozen in the gas phase. As pointed out by Ziering[6], this assumption seems questionable in view of the high pressures and temperatures of interest. The frozen assumption appears to stem more from historical precedent (i.e., Dolton[4]) than from any physical rationale.

The previous analysis [Eqs. (1) through (13)] remains valid for this subsection, but the reactions are recast in somewhat different form. The carbon-oxygen species and the oxygen and nitrogen dissociation reactions are assumed to be in equilibrium

$$\begin{aligned} CO + O &\rightleftharpoons CO_2 && K_{P_{13}} \\ O_2 &\rightleftharpoons 2\,O && K_{P_7} \\ N_2 &\rightleftharpoons 2\,N && K_{P_8} \end{aligned} \qquad (28)$$

Note that the carbon monoxide dissociation reaction has been deleted in keeping with the requirement that gas-phase reactions involving free carbon are prohibited by the frozen assumption.

The equilibrium relationships are given by

$$P_{CO_2} = \alpha_{13} P_O P_{CO}$$

$$P_{O_2} = \alpha_7 P_O^2$$

$$P_N = \alpha_8 P_{CN} \qquad (29)$$

where the α coefficients are defined by

$$\alpha_{13} \equiv K_{P_{13}} \qquad \alpha_7 \equiv \frac{1}{K_{P_7}} \qquad \alpha_8 \equiv \sqrt{\alpha_1^* K_{P_8}} \qquad (30)$$

The carbon-nitrogen species are assumed to be in gas-phase equilibrium with each other. This yields

$$C_2N_2 \rightleftharpoons 2\ CN$$

$$C_4N_2 \rightleftharpoons 2\ C_2N$$

$$N_2 + C_4N_2 \rightleftharpoons 4\ CN \qquad (31)$$

Since there are four carbon-nitrogen species present in the system, a fourth reaction is required to close the formulation. There is no way to write a fourth linearly independent expression involving the species of Eq. (31). Therefore, the required expression must involve any of those species and carbon. Since gas-phase reactions involving the carbon sublimation species are prohibited, the fourth equation must be a heterogeneous nitridization reaction. Therefore, we require the following reaction to be in equilibrium:

$$2C^* + N_2 \rightleftharpoons 2\ CN \qquad (32)$$

As indicated in Subsection II-B, Eqs. (31) and (32) are exactly equivalent to the full set of heterogeneous reactions of Eqs. (22). Therefore, we adopt Eqs. (23) through (25) for the formulation of this subsection.

The carbon dissociation reactions of Eq. (17) are deleted and replaced by the following expressions:

$$\frac{\dot{m}_{C_i}}{\rho_e u_e C_H} = (1 + B') K_{C_{i_w}} - K_{C_{i_e}} ; \qquad i=1-5 \tag{33}$$

The frozen species equations are obtained from the species continuity equation and the analogy between mass and heat transfer (for equal diffusion coefficients and unity Lewis and Prandtl numbers).

Casting Eq. (33) in terms of partial pressures and combining with the Knudsen-Langmuir Eq. (7) yields

$$\frac{PM}{1 + B'} = \frac{\rho_e u_e C_H M_{C_i} P_{C_i}}{\beta_{C_i} \sqrt{\frac{M_{C_i}}{2\pi RT}} \left(P^v_{C_i} - P_{C_i}\right) + \rho_e u_e C_H K_{C_{i_e}}} \tag{34}$$

Combining the oxygen mass balance of Eq. (5) and the summation of partial pressures [Eq. (6)] and using Eqs. (24), (29), and (30) yields

$$\begin{aligned} & A P_O^2 + B P_O + C = 0 \\ & P_{C_O} = 2\lambda - P_O - \left(\frac{PM}{1 + B'}\right) \frac{\tilde{K}_{O_e}}{16} \\ & A \equiv 16 \left(\alpha_7 - \alpha_{13}\right) > 0 \\ & B \equiv \alpha_{13} \left(32\lambda - \frac{PM}{1 + B'} \tilde{K}_{O_e}\right) > 0 \end{aligned} \tag{35}$$

$$C \equiv \left(16\lambda - \frac{PM}{1+B'} \tilde{K}_{O_e} \right) < 0$$

$$\lambda \equiv P - \sum P_{C_i} - (1 + \alpha_4^* + \alpha_8) P_{CN} - (\alpha_1^* + \alpha_2^* + \alpha_3^*) P_{CN}^2 + \\ - \frac{PM}{1+B'} \frac{\tilde{K}_{I_e}}{M_I} \qquad \text{(35 cont.)}$$

The nitrogen mass balance of Eq. (5) becomes

$$28(\alpha_1^* + \alpha_2^* + \alpha_3^*) P_{CN}^2 + 14(1 + \alpha_4^* + \alpha_8) P_{CN} = \frac{PM}{1+B'} \tilde{K}_{N_e} \qquad (36)$$

The carbon mass balance of Eq. (5) is

$$\frac{PM}{1+B'} \left(B' + \tilde{K}_{C_e} \right) = 12\left(1 + \alpha_{13} P_O\right) P_{CO} + (12 + 24\alpha_4^*) P_{CN} + \\ + (24\alpha_2^* + 48\alpha_3^*) P_{CN}^2 + \sum M_{C_i} P_{C_i} \qquad (37)$$

An examination of this system of equations indicates that the carbon species partial pressures cannot be evaluated solely from a guessed value of one of them. This is a consequence of replacing the equilibrium expressions of Eq. (17) by the frozen expressions of Eq. (33). This considerably complicates the numerical solution procedure, requiring a double iteration involving the blowing heat flux and one of the carbon partial pressures. The outer iteration loop consists of guessing a value for $\rho_e u_e C_{H'}$ solving the inner iteration loop for B' and checking the guess against Eq. (12).

For a supplied value of $\rho_e u_e C_{H'}$ the iteration procedure for the inner loop is described by the following: Guess a value for P_{C_3} and solve Eq. (34) for $PM/(1+B')$. Since Eq. (34) is valid for every sublimation species, it

may be resolved for the remaining P_{C_i} using the value of $PM/(1+B')$ obtained from the guess for P_{C_3}. Next, Eq. (36) is solved for P_{CN} and Eq. (35) for P_O and P_{CO}. The mass transfer parameter B' is then calculated from Eq. (37) and checked against the value obtained from Eq. (11). If the two values of B' do not agree, a new guess is made for the C_3 partial pressure, and the process repeated until the iteration converges. The guessed value of P_{C_3} is constrained by requiring it to be less than the C_3 vapor pressure, and by the requirement that the B and C coefficients of Eq. (35) have the indicated signs. If B is negative, the guessed value for P_{C_3} is too large, whereas it is too small if C is positive.

D. VAPORIZATION OF MOLTEN CARBON

As indicated previously, the major objective of this report is to examine the impact of various assumptions concerning the chemical state of the system upon the predicted ablation. Thus, in Subsections II-A through II-C, the influence of the limiting reaction rates (i.e., fast-slow) was examined. However, in all cases, it was assumed that carbon sublimed from a solid surface. In this subsection, we shall examine the influence of the surface state (i.e., solid or liquid phase) on the ablation formulation. In other words, it will be assumed that the carbon vaporization reactions occur from a liquid carbon surface.

Kratsch[3] used an equilibrium analysis to calculate the liquid layer mass loss and obtained values about an order of magnitude larger than the comparable recession due to sublimation from a solid surface. It is not clear exactly how these large recession rates were obtained, but one possibility might be that the melt layer was mechanically removed from the surface by aerodynamic forces. Since recession rates of this magnitude are not indicated by experimental data, some doubt must be cast on the validity of the Kratsch analysis. The lower-bound limiting assumption is that the melt layer remains in place, and the mass loss is simply the vaporization rate from the liquid surface. If the melt layer is sufficiently thin, then

viscous forces and surface adhesion will resist mechanical removal and flowing of the liquid layer. This report will assume that the liquid layer is thin enough such that it does not flow and is not removed by aerodynamic forces.

It should be apparent, therefore, that the analysis of the vaporization from a liquid surface is similar to the sublimation analysis from a solid surface. The only difference is that the properties of the solid carbon are replaced by the properties of liquid carbon. In particular, the equilibrium vapor pressure existing over a liquid surface is different than that existing over a solid surface. Thus, the vapor pressure for solid carbon must be replaced by the liquid value. The vapor pressure for both phases is obtained from Appendix A.

The phase state of the surface probably influences other aspects of the ablation, such as the oxidation and nitridization reaction rates and the values for the vaporization coefficients. Since the partial pressures of atomic and molecular oxygen are vanishingly small for the melt temperatures of interest, the oxidation reactions are insignificant. The situation with respect to the vaporization coefficients and nitridization reactions is not as obvious. In the absence of any other information, the same set of vaporization coefficients will be used for both the solid and liquid phases. The use of the equilibrium assumption for the heterogeneous nitridization reactions yields the same inconsistencies as were encountered with the solid carbon surface. Therefore, the slow nitridization assumption is utilized.

In summary, the analysis for the vaporization of a carbon melt layer is identical to that of Subsection II-A, with the correct vapor pressure law for liquid-gas equilibrium.

E. SURFACE ENERGY BALANCE

The analysis of the preceding subsections treated the surface temperature as a known quantity. Although a prescribed temperature is a common boundary condition for boundary layer calculations, most ablation analyses require the determination of the surface temperature as part of the solution. The temperature is obtained by satisfying the surface energy balance which equates the net aerodynamic surface heat flux to the energy conducted into the interior of the body.

The surface energy balance may be expressed as

$$\dot{q}_C = \rho_e u_e C_{H_0} \left(\frac{C_H}{C_{H_0}} \right) \left[H_R - H_w - B' (H_w - H_S) \right] - \sigma \epsilon T_w^4$$

$$H_w = \sum K_i h_i \qquad (38)$$

where $\dot{q}_C$ denotes the energy conducted into the body and H_S is the enthalpy of the surface phase (liquid or solid) supplied by the Appendix.

In principle, a knowledge of the interior temperature field is required to evaluate $\dot{q}_C$, thereby coupling the in-depth material response calculation to the surface mass transfer calculation. If the conduction heat transfer can be expressed solely in terms of the surface temperature, the mass transfer calculation may be uncoupled from the in-depth material response, resulting in a considerable simplification. This uncoupling is usually accomplished by invoking the steady-state assumption to evaluate the conduction heat transfer. It is the purpose of this subsection to present an alternate model for the conduction heat transfer which includes the influence of the time scale.

It is assumed that the conduction may be represented as a one-dimensional process normal to the surface. It is also assumed that the body dimension normal to the surface is much larger than the thermal penetration depth for the time scale of interest, such that the body may be represented as a semi-infinite domain.

The conduction equation may be written in a coordinate system which translates with the surface as it ablates. This yields

$$\rho C_p \frac{\partial T}{\partial t} - \rho C_p \dot{S} \frac{\partial T}{\partial x} = \frac{\partial}{\partial x}\left(K \frac{\partial T}{\partial x}\right) \tag{39}$$

Integrating from x = 0 (surface) to x = ∞ and assuming constant material properties yield

$$\dot{q}_C \equiv \left(-K \frac{\partial T}{\partial x}\right)_{x=0} = \dot{m} C_p (T_w - T_B) + \rho C_p \int_0^\infty \frac{\partial T}{\partial t}\, dx \tag{40}$$

where T_B is the bulk temperature of the in-depth material.

The first term of this expression is recognized as the steady-state approximation. It is apparent that the steady-state assumption will be valid if the time scale is large enough so that the integral term is negligible. However, if the time scale is small or the recession rate ($\dot{S}$) is low, then the integral term dominates, and the steady-state assumption is quite poor. In order to introduce the time scale into the problem, the integral term must be approximated in some manner. This is accomplished by using the solution of Carslaw and Jaeger[11] for a semi-infinite domain (of a single phase) with constant surface temperature and recession rate. This yields

$$\dot{q}_C = \dot{m} C_p (T_w - T_B) \left\{ 1 - \frac{1}{2} \mathrm{ERFC}\left(\frac{\dot{S}}{2}\sqrt{\frac{t}{\sigma}}\right) + \frac{\mathrm{EXP}\left[-\left(\frac{\dot{S}}{2}\sqrt{\frac{t}{\sigma}}\right)^2\right]}{2\sqrt{\pi}\left(\frac{\dot{S}}{2}\sqrt{\frac{t}{\sigma}}\right)} \right\} \tag{41}$$

[11] Carslaw, H. S. and J. C. Jaeger, Conduction of Heat in Solids, Oxford University Press, 1959, p. 388.

This expression is plotted in Fig. 1 where it is apparent that the requirement for the steady-state approximation to be valid is given by

$$\frac{\dot{S}}{2}\sqrt{\frac{t}{\sigma}} > 1 \tag{42}$$

Note that Eq. (41) possesses the correct limiting behavior as the time and/or recession rate vanishes, whereas the steady-state model is clearly incorrect.

Thus, for a specified value of time, Eq. (41) may be solved with the surface energy balance to yield the temperature and recession rate. The time scale is simply chosen to be the elapsed time from the initiation of the heating pulse. It is felt that the introduction of the time scale in this manner should substantially increase the accuracy for applications in which the steady-state approximation is invalid, while retaining the computational simplicity associated with uncoupling the in-depth response from the surface mass transfer.

Equations (38) through (42) provide all the necessary information to analyze the ablation from a solid carbon surface. If, however, the solid carbon changes phase by melting, additional information is required. The transient solution required to obtain Eq. (41) is only valid for a solid carbon body and is not applicable for the carbon melt layer problem. Unfortunately, the analogous transient conduction solution for a two-phase semi-infinite body, with a receding surface, does not exist. Therefore, the analysis of the melt layer problem will utilize the steady-state conduction assumption.

The expression of Eq. (40) is also valid for the situation where a phase change occurs in depth. Thus, the steady-state conduction assumption (for either a single phase or two phases) may be expressed in terms of enthalpies as

$$\dot{q}_C = \dot{m}\,(H_S - H_B) \tag{43}$$

where H_B is the enthalpy of solid carbon at the bulk temperature.

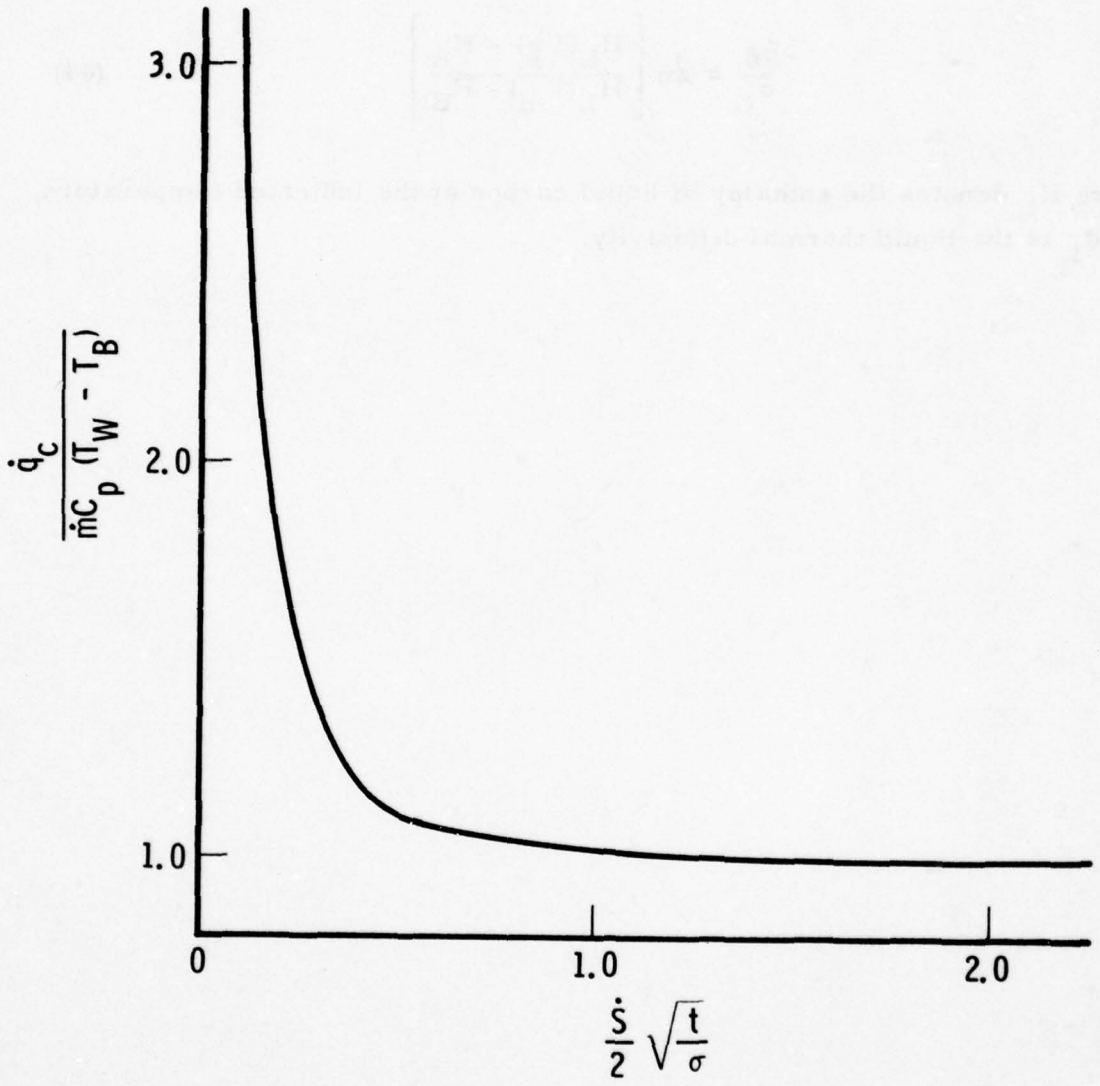


Fig. 1. Influence of Time Scale and Recession Rate on the Steady-State Conduction Assumption

The thickness of the liquid carbon layer is also required to check the assumption that the melt layer is thin. The steady-state conduction solution yields the following result for the melt layer thickness (i.e., δ)

$$\frac{\dot{S}\delta}{\sigma_L} = \ell n \left[\frac{H_L(T_w) - H_B}{H_L(T_m) - H_B} \right] \tag{44}$$

where H_L denotes the enthalpy of liquid carbon at the indicated temperature, and σ_L is the liquid thermal diffusivity.

III. RESULTS AND DISCUSSION

The assumptions utilized in the analysis are examined in this section, the various models are compared to each other, and comparisons are made with experimental data. In Subsection III-A, calculations are presented for the kinetically controlled oxidation regime, and the impact of uncoupling the boundary layer calculation from the surface mass transfer calculation is examined. In Subsection III-B, calculations utilizing the slow nitridization assumption are presented. Comparisons are made with the fast nitridization assumption in Subsection III-C and the frozen sublimation species in III-D. Carbon melt layer calculations are shown in Subsection III-E, and the influence of the steady-state conduction assumption is examined in Subsection III-F. Finally, some comparisons with experimental ablation data are presented in Subsection III-G.

Before proceeding, some ground rules for the computations must be established. First, all the calculations of this report are for air environments. Thus, the boundary layer edge mass fractions for the elements and the carbon species (required for the frozen assumption) are given by

$$\tilde{K}_{O_e} = 0.232 \qquad \tilde{K}_{N_e} = 0.768 \qquad \tilde{K}_{I_e} = 0$$

$$\tilde{K}_{C_e} = 0 \qquad K_{C_{i_e}} = 0 \tag{45}$$

Although the one percent mass fraction of argon present in the atmosphere could be included as the inert species, its effect is negligible and is usually ignored.

As indicated earlier, it is not the intention of this report to examine the influence of species property variations upon the predicted mass transfer. Therefore, a fixed set of species data was used throughout. With one exception, the JANNAF free energy functions and nominal heats of formation were utilized. However, the JANNAF values for the C_3 molecule are generally believed to be in error. Accordingly, the recent calculation of Hansen and Pearson[12], as curve fit by Pearson and Davy[13], were used for the C_3 free energy function. Note that these results are essentially identical to the earlier values obtained by Straus and Thiele[14]. The Wachi and Gilmartin[15] heat of formation was adopted for C_3. A total of five carbon sublimation species was included in the calculations, and the JANNAF data was used for the other four species.

According to the JANNAF data, the only major uncertainty in the species of interest is the C_2N heat of formation. That is, JANNAF quotes a nominal heat of formation of 131.9 kcal/mol, with a possible variation of ±30 kcal/mol. This represents a tremendous spread in the predicted C_2N mass fraction; it varies from being the dominant species in the system (for the smallest heat or formation) to only a trace species (for the largest heat of formation). A more recent value for the C_2N heat of formation was given by Meyer and Setser[16] as 184 kcal/mol. It is clear that additional work is required to narrow this range of values. In any event, the nominal JANNAF value was used in this report.

---

[12] Hansen, C. F. and W. E. Pearson, "A Quantum Model for Bending Vibrations and Thermodynamic Properties of C_3," Canadian Journal of Physics, 51, 1973.

[13] Pearson, W. E. and W. C. Davy, "New Thermodynamic Functions for the C_3 Molecule," AIAA Journal, 11(8), August 1973.

[14] Strauss, H. L. and E. Thiele, "Thermodynamics of C_3 General Methods for Nonrigid Molecules at High Temperature," Journal of Chemical Physics, 46(7), April 1967.

[15] Wachi, F. M. and D. E. Gilmartin, "Heat of Formation and Entropy of C_3 Molecule," Report No. TR-0172(2250-40)-7, The Aerospace Corporation, El Segundo, Calif., May 1972.

[16] Meyer, J. A. and D. W. Setser, "Chemiluminescence from the Reaction of Oxygen Atoms with Dicyanoacetylene," Journal of Physical Chemistry, 74, 1970, p. 3452.

There remains considerable uncertainty about the vaporization coefficients for the carbon species, with some investigators claiming values close to unity and others (see Dolton[4]) obtaining values small compared to unity. For unity vaporization coefficients, the nonequilibrium formulation yields results quite similar to the equilibrium values (see Baker[5]). The vaporization coefficients used by Dolton yield significant departures from equilibrium and are the values used herein. These values are given as

$$\beta_C = 0.24 \qquad \beta_{C_2} = 0.50 \qquad \beta_{C_3} = 0.023$$

$$\beta_{C_4} = 0.25 \qquad \beta_{C_5} = 0.0019 \tag{46}$$

Note that there is no reason to believe that the vaporization coefficients are independent of temperature. They are invariably assumed constant due to a lack of data on the influence of temperature. Similarly, the vaporization coefficients from a liquid carbon surface would not be expected to be the same as those from a solid surface. It has been postulated that vaporization from a liquid surface should take place more readily than from a solid surface and, therefore, that the liquid vaporization coefficients should tend towards unity. However, Hirth[17] suggests that liquids with polymeric vapor species should have values less than unity. In the absence of any other information, it is assumed that the Dolton vaporization coefficients also apply to liquid carbon.

A. KINETICALLY CONTROLLED OXIDATION

The objectives of this subsection are twofold. First, to determine the applicability of the iteration scheme of Subsection II-A at low temperatures and second, to compare the results with an exact boundary layer calculation. The choice of the C_3 partial pressure as the iteration parameter was based on the fact that it is the dominant carbon species at elevated temperatures.

[17] Hirth, J. P., "Evaporation and Sublimation Mechanisms," The Characterization of High Temperature Vapors, J. L. Margrave (ed.), John Wiley & Sons, Inc., New York, 1967.

However, in the low-temperature oxidation regime it exists only as a trace species. In some instances, the use of a trace species as an iteration parameter can lead to very slow convergence or nonconvergence. No difficulties of this sort were encountered in the calculations reported herein.

As indicated in Section II, several assumptions were used to uncouple the boundary layer calculation from the surface mass transfer calculation. Specifically, the assumption of unity Prandtl and Lewis numbers and equal diffusion coefficients were employed to relate the wall and edge elemental mass fractions [Eq. (3)]. In order to assess the impact of these assumptions, comparison is made with an exact boundary layer calculation[18] which does not utilize such assumptions.

The case of interest consists of a stagnation point calculation at moderate pressure over a range of temperature up to the CO diffusion limit. The oxidation reaction involves only molecular oxygen and is characterized by two reaction rates, designated as slow and fast. The reaction rates and reaction order are given by

$$\text{Slow reaction:} \quad K_{O_2} = 4.47 \times 10^4 \, e^{-42300/RT}$$

$$\text{Fast reaction:} \quad K_{O_2} = 6.73 \times 10^8 \, e^{-44000/RT}$$

$$\text{Reaction order:} \quad n_{O_2} = 0.50 \tag{47}$$

The values of $\rho_e u_e C_H$ required for the formulation of Subsection II-A were obtained from the exact solution. Thus, the blowing model [Eqs. (12) or (13)] does not enter into the comparison.

---

[18] Bernstein, H. and J. R. Baron, "Stability Characterization of Refractory Materials under High Velocity Atmospheric Flight Conditions, Part IV, Volume II, Calculation of the General Surface Reaction Problem," AFML TR-69-84, December 1969.

The comparison is shown in Fig. 2 where it is apparent that the exact and approximate solution differ by less than 10 percent. It is concluded, therefore, that the assumptions used to uncouple the boundary layer and mass transfer calculations are valid. In fact, the uncertainties in the oxidation kinetics will swamp any of the uncoupling assumptions.

B. SLOW NITRIDIZATION CALCULATIONS

In the previous subsection, the computation scheme of Subsection II-A was used to obtain results in the low-temperature oxidation regime. Since carbon-nitrogen compounds and carbon sublimation species are insignificant at low temperatures, the impact of the assumptions of Subsections II-A through II-C are unrecognizable in the oxidation regime. In order to distinguish between the various reaction rate assumptions, a set of calculations is presented for the sublimation regime. Since the atomic and molecular oxygen partial pressures vanish at high temperatures, the choice of reaction rate for the oxidation reaction exerts negligible influence on the results.

The mass transfer parameter is presented in Figs. 3 through 5 for three pressures and a range of nonblowing heat transfer coefficients. The calculations used the laminar blowing expression of Eq. (12) and the Dolton vaporization coefficients. For comparative purposes, the equilibrium values are also shown. As expected, as the pressure increases, larger values of heat flux are required to obtain significant departures from the equilibrium values.

C. COMPARISON OF FAST AND SLOW NITRIDIZATION ASSUMPTIONS

The B' calculations for the fast and slow nitridization assumptions are compared in Figs. 6 through 9 for several pressures and nonblowing convective heat fluxes. The laminar blowing expression of Eq. (12) and the Dolton vaporization coefficients were utilized for the calculations, and the gas-phase reactions were in equilibrium, subject to the restrictions required for the fast nitridization assumption.

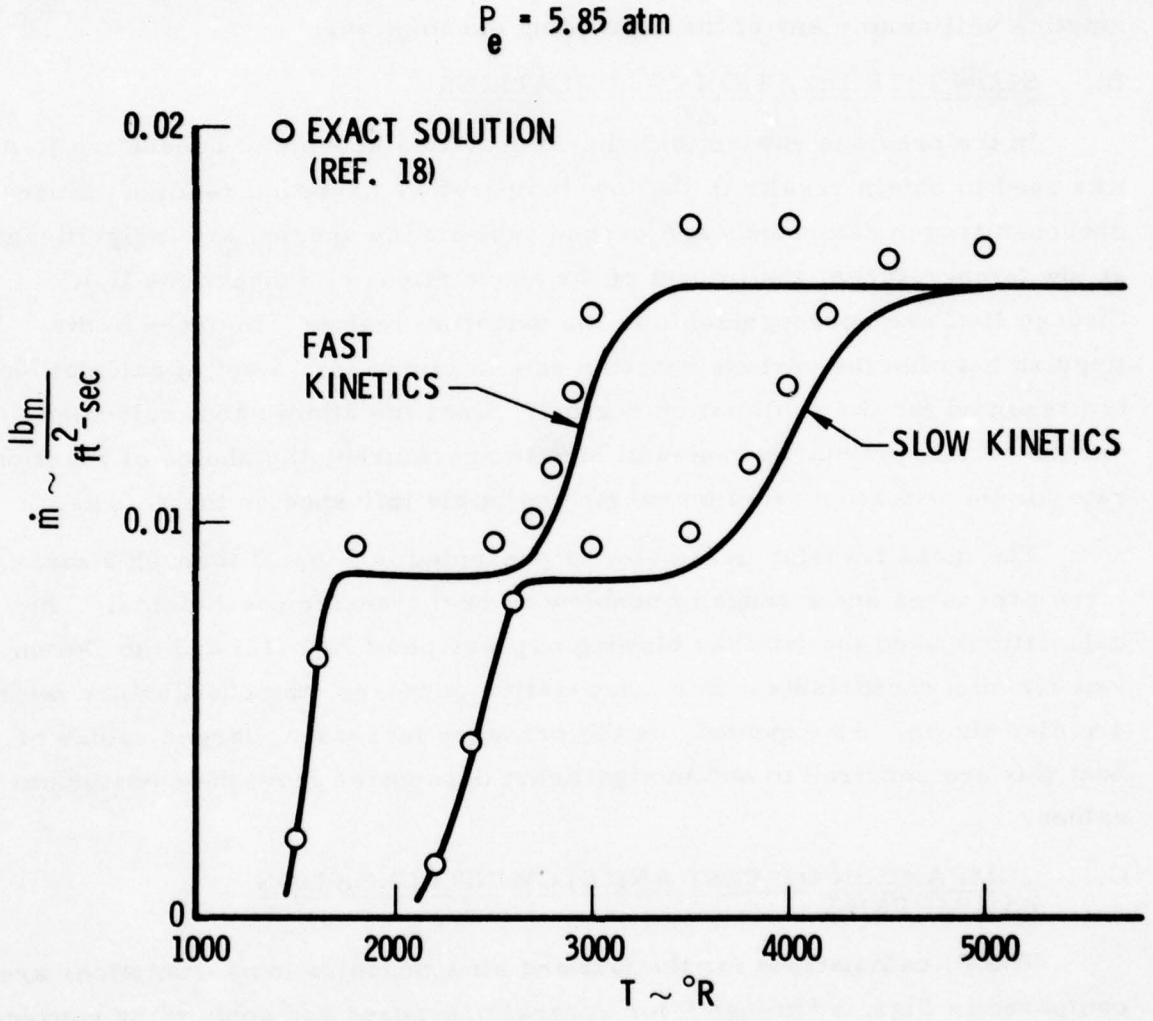


Fig. 2. Comparison with Exact Calculations for Oxidation Mass Loss

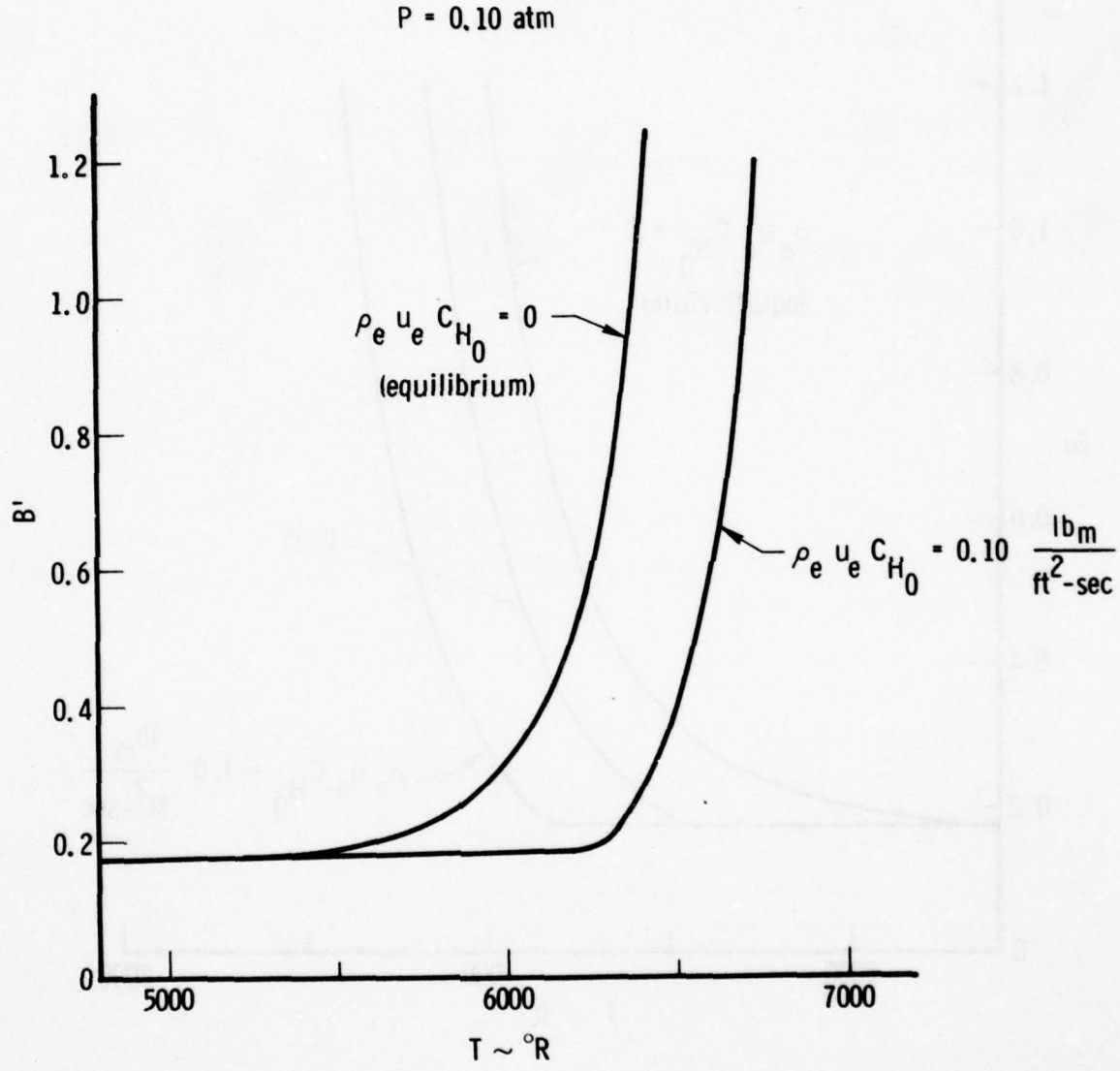


Fig. 3. Slow Nitridization Calculations
(P = 0.10 atm)

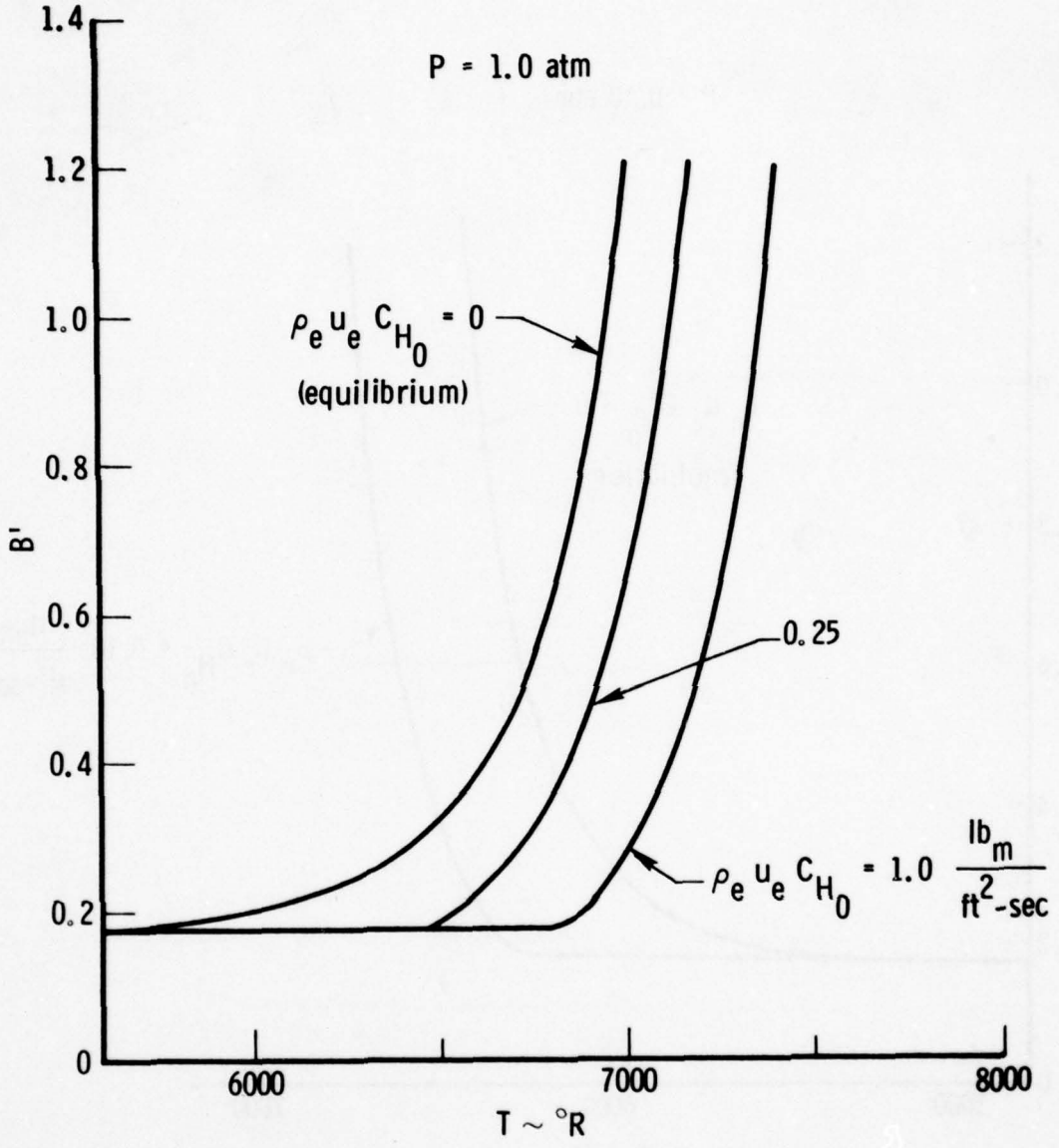


Fig. 4. Slow Nitridization Calculations
(P = 1.0 atm)

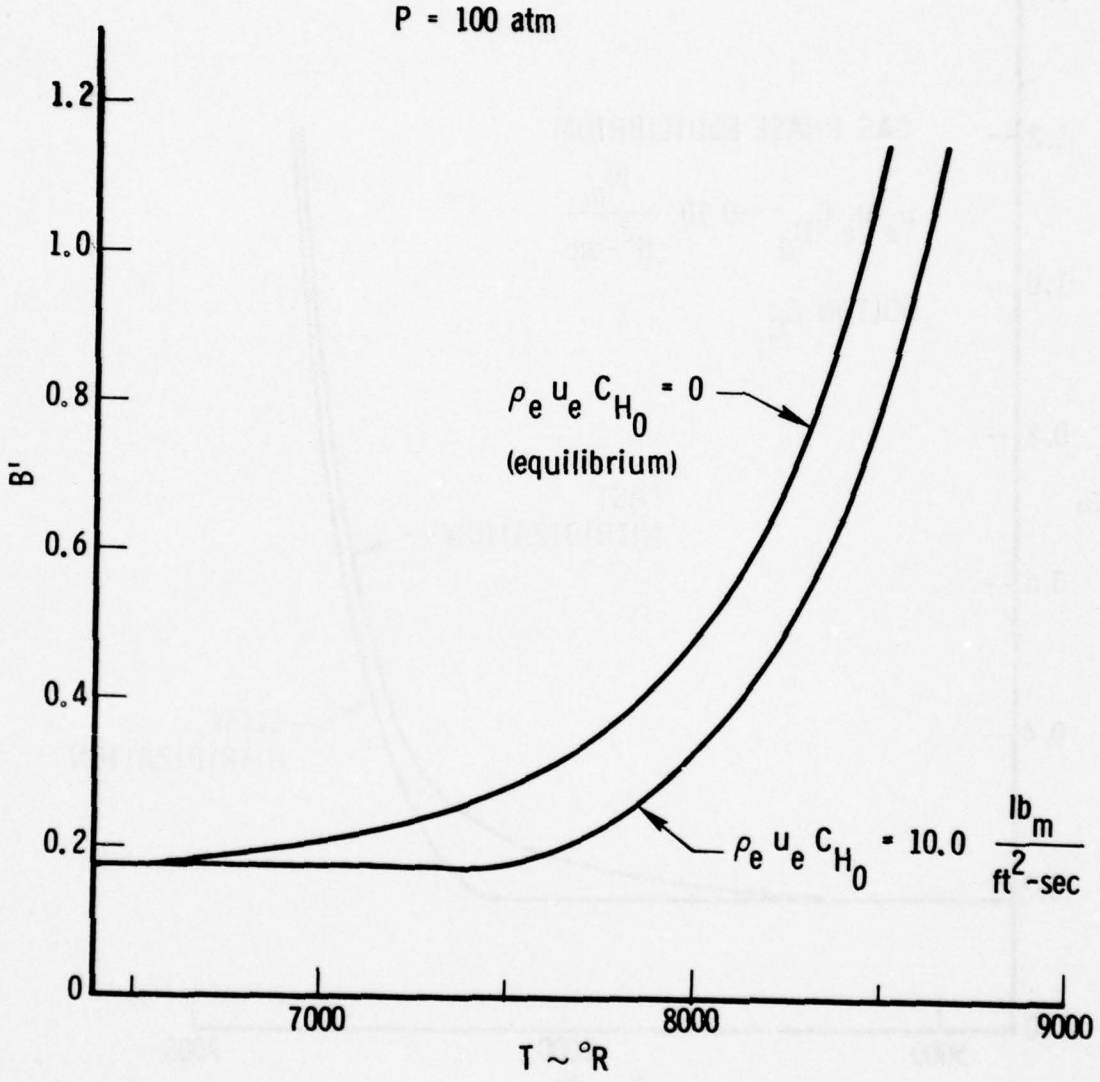


Fig. 5. Slow Nitridization Calculations
(P = 100 atm)

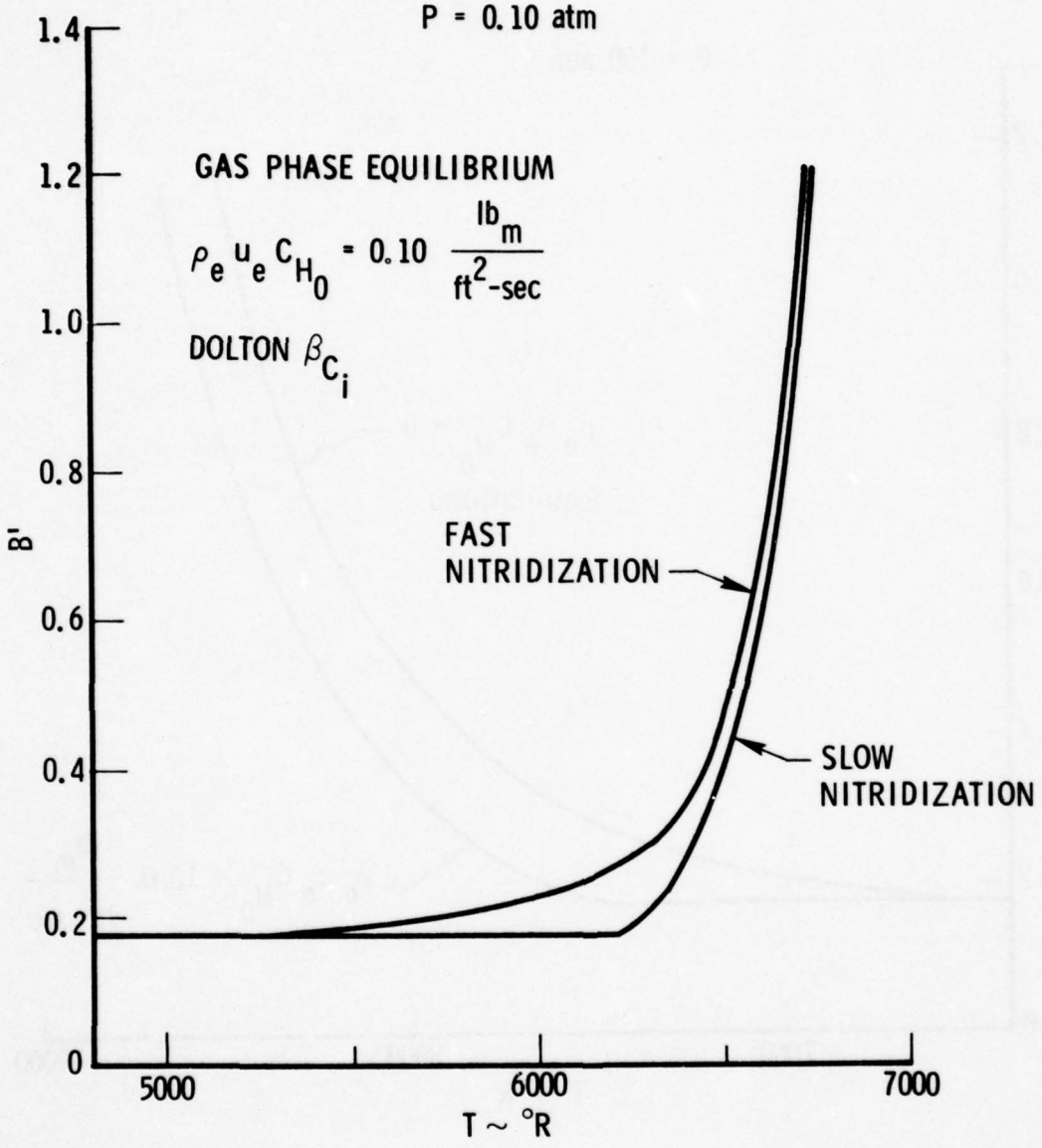


Fig. 6. Influence of Heterogeneous Nitridization Reactions (P = 0.10 atm)

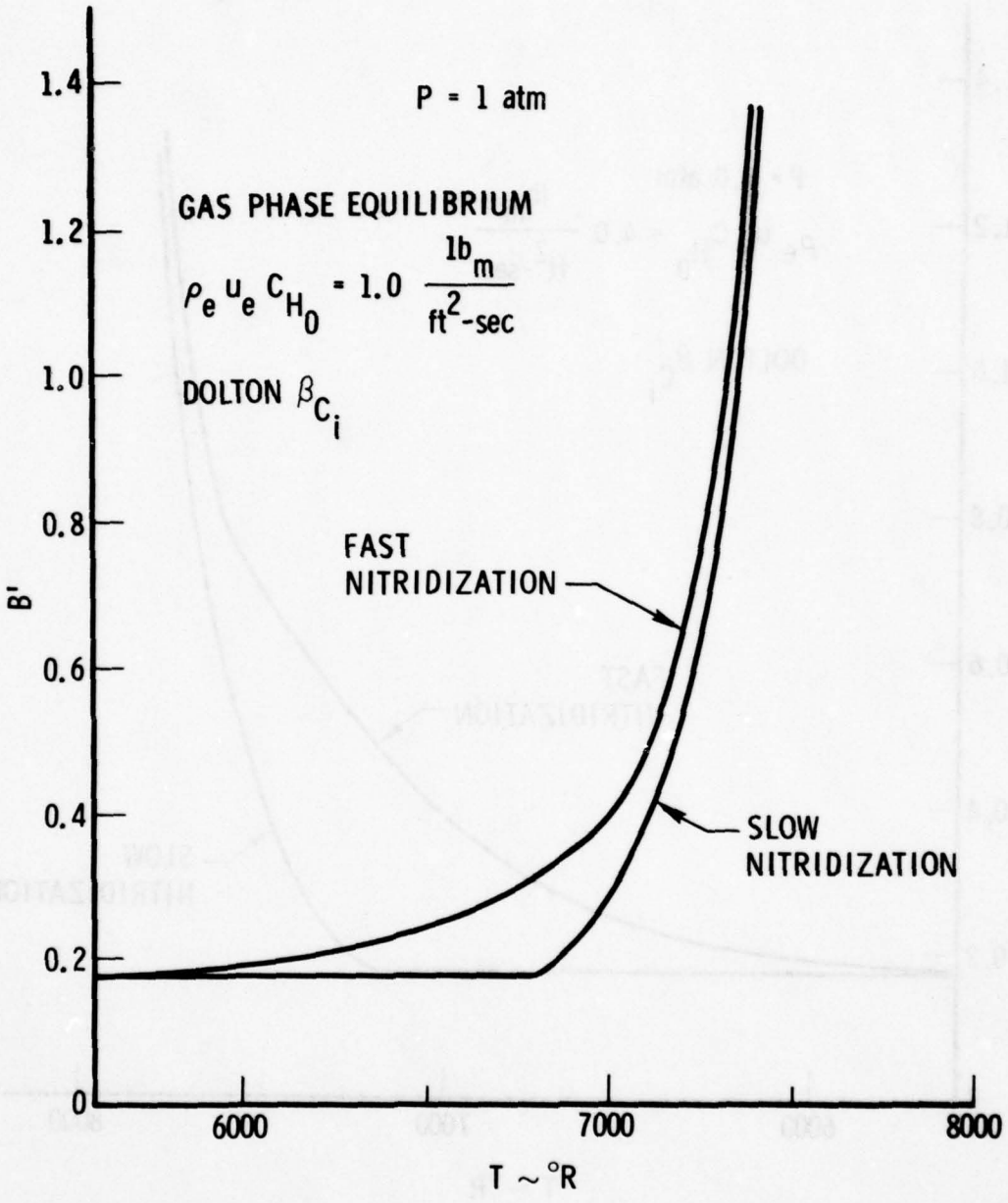


Fig. 7. Influence of Heterogeneous Nitridization Reactions (P = 1.0 atm)

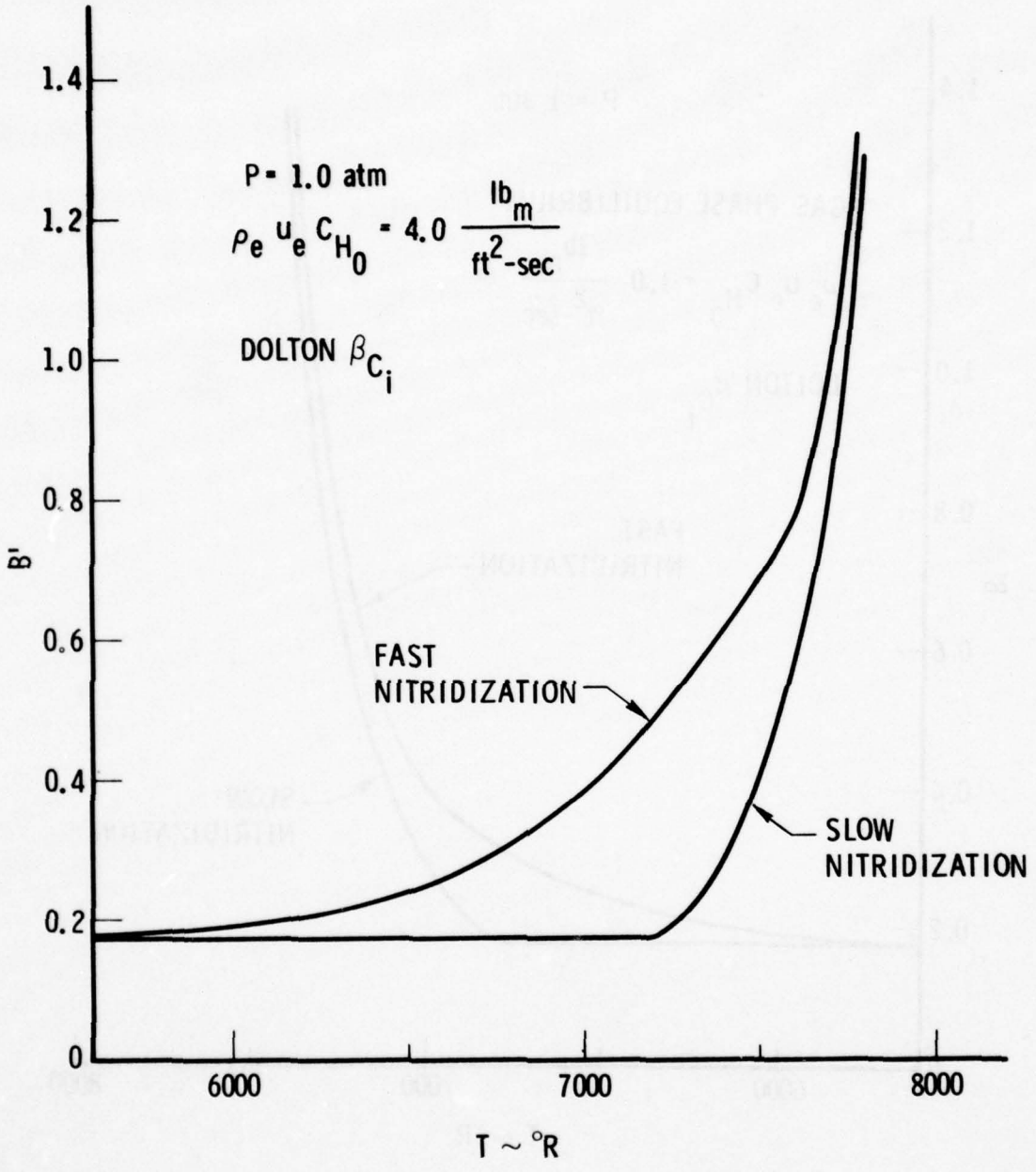


Fig. 8. Influence of Heterogeneous Nitridization Reactions (P = 1.0 atm)

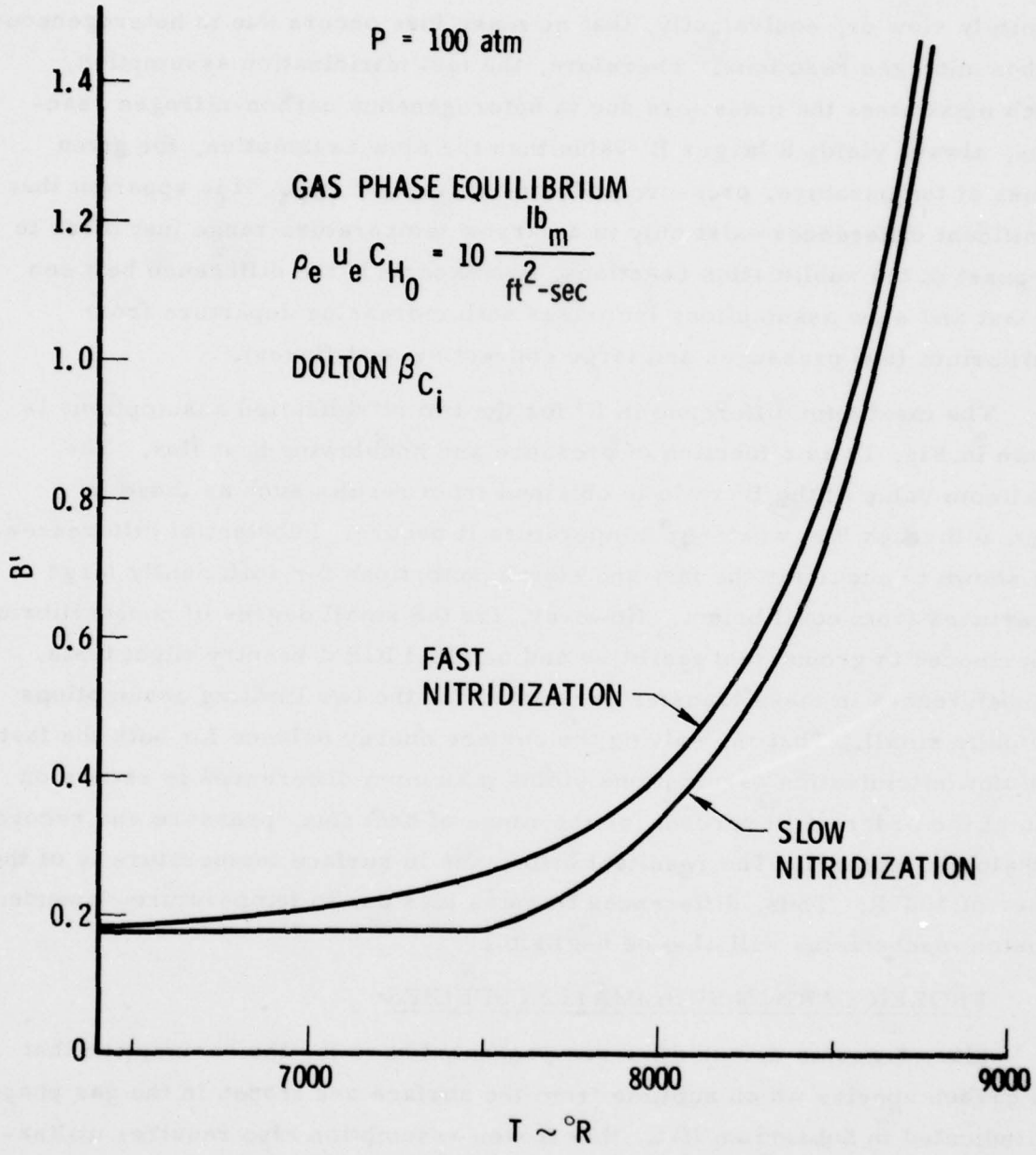


Fig. 9. Influence of Heterogeneous Nitridization Reactions (P = 100 atm)

The term "slow nitridization," in the context used herein, means infinitely slow or, equivalently, that no mass loss occurs due to heterogeneous carbon-nitrogen reactions. Therefore, the fast nitridization assumption, which maximizes the mass loss due to heterogeneous carbon-nitrogen reactions, always yields a larger B' value than the slow assumption, for given values of temperature, pressure and convective heat flux. It is apparent that significant differences exist only in a narrow temperature range just prior to the onset of the sublimation reactions. As expected, the difference between the fast and slow assumptions increases with increasing departure from equilibrium (low pressures and large convective heat fluxes).

The maximum difference in B' for the two nitridization assumptions is shown in Fig. 10 as a function of pressure and nonblowing heat flux. The maximum value of the B' ratio is obtained from results such as those in Figs. 6 through 9 at whatever temperature it occurs. Substantial differences are shown to occur for the fast and slow assumptions for sufficiently large departures from equilibrium. However, for the small degree of nonequilibrium experienced in ground test facilities and nominal ICBM reentry flight tests, the differences in mass transfer parameter for the two limiting assumptions are quite small. That is, solving the surface energy balance for both the fast and slow nitridization assumptions yields maximum differences in recession rate of the order of 10 percent for the range of heat flux, pressure and recovery enthalpy of interest. The resultant difference in surface temperature is of the order of $100^{\circ}R$. Thus, differences in mass loss due to temperature-dependent erosion mechanisms will also be negligible.

D. FROZEN CARBON SUBLIMATION SPECIES

Mass transfer calculations are presented here for the assumption that the carbon species which sublime from the surface are frozen in the gas phase. As indicated in Subsection II-C, this frozen assumption also requires utilization of the fast nitridization assumption for the heterogeneous carbon-nitrogen

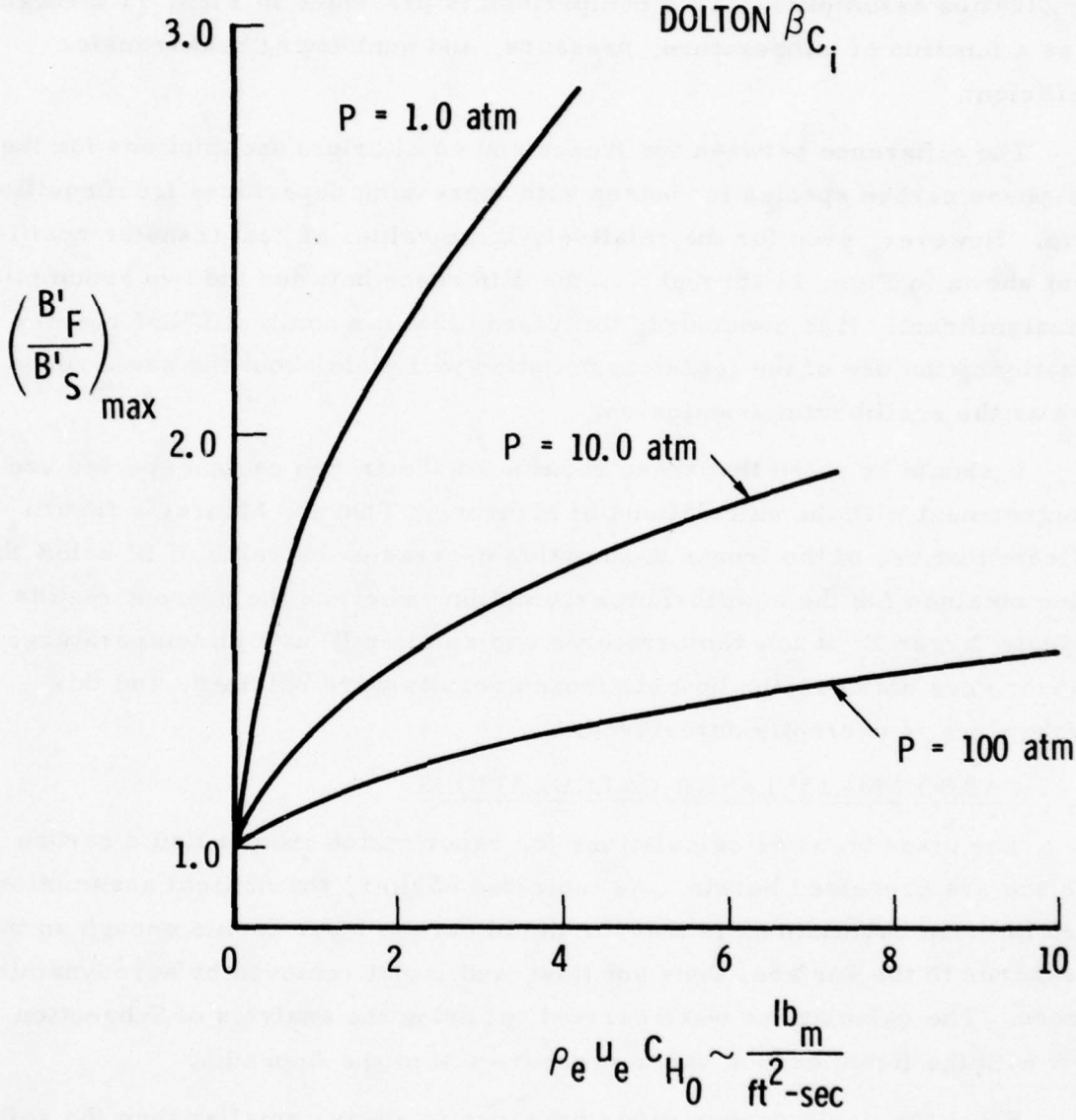


Fig. 10. Maximum B' Difference for Fast and Slow Nitridization Assumptions

reactions. Therefore, the influence of the frozen gas-phase reaction is seen by comparison with the equilibrium gas-phase calculations with the fast nitridization assumption. This comparison is presented in Figs. 11 through 13 as a function of temperature, pressure, and nonblowing heat transfer coefficient.

The difference between the frozen and equilibrium assumptions for the gas-phase carbon species increases with increasing departures from equilibrium. However, even for the relatively large values of heat transfer coefficient shown in Figs. 11 through 13, the difference between the two assumptions is insignificant. It is concluded, therefore, that for nominal ICBM reentry situations, the use of the frozen assumption will yield about the same recession as the equilibrium assumption.

It should be noted that these results for the frozen carbon species are in disagreement with the calculations of Maurer[2]. That is, Maurer's results indicate that use of the frozen assumption decreases the value of B' below the value obtained for the equilibrium assumption, whereas the present results indicate larger B' at low temperatures and smaller B' at high temperatures. Maurer does not describe how his frozen results were obtained, and this discrepancy is currently unresolved.

E. CARBON MELT LAYER CALCULATIONS

The mass transfer calculations for vaporization from a liquid carbon surface are presented herein. As indicated earlier, the critical assumption used in these calculations is that the liquid carbon layer is thin enough so that it adheres to the surface, does not flow, and is not removed by aerodynamic forces. The calculations were carried out using the analysis of Subsection II-A with the liquid carbon vapor pressure law of the Appendix.

Since the liquid carbon vapor pressure is always smaller than the solid carbon vapor pressure, the mass transfer from the liquid surface should be less than that from the solid surface at the same conditions. This is evident in Figs. 14 and 15 where the equilibrium values of B' are presented for two

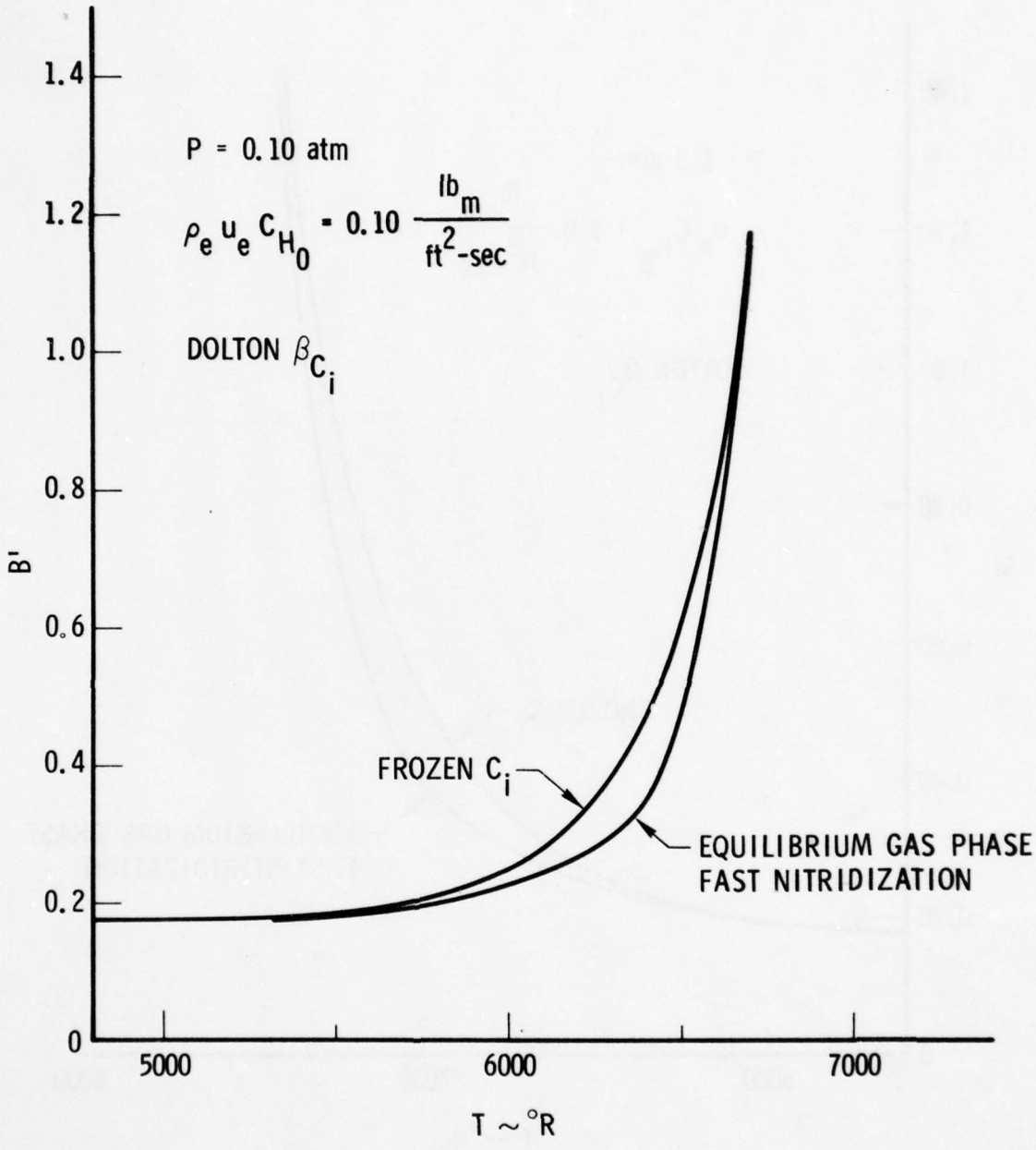


Fig. 11. Influence of Frozen Sublimation Species (P = 0.10 atm)

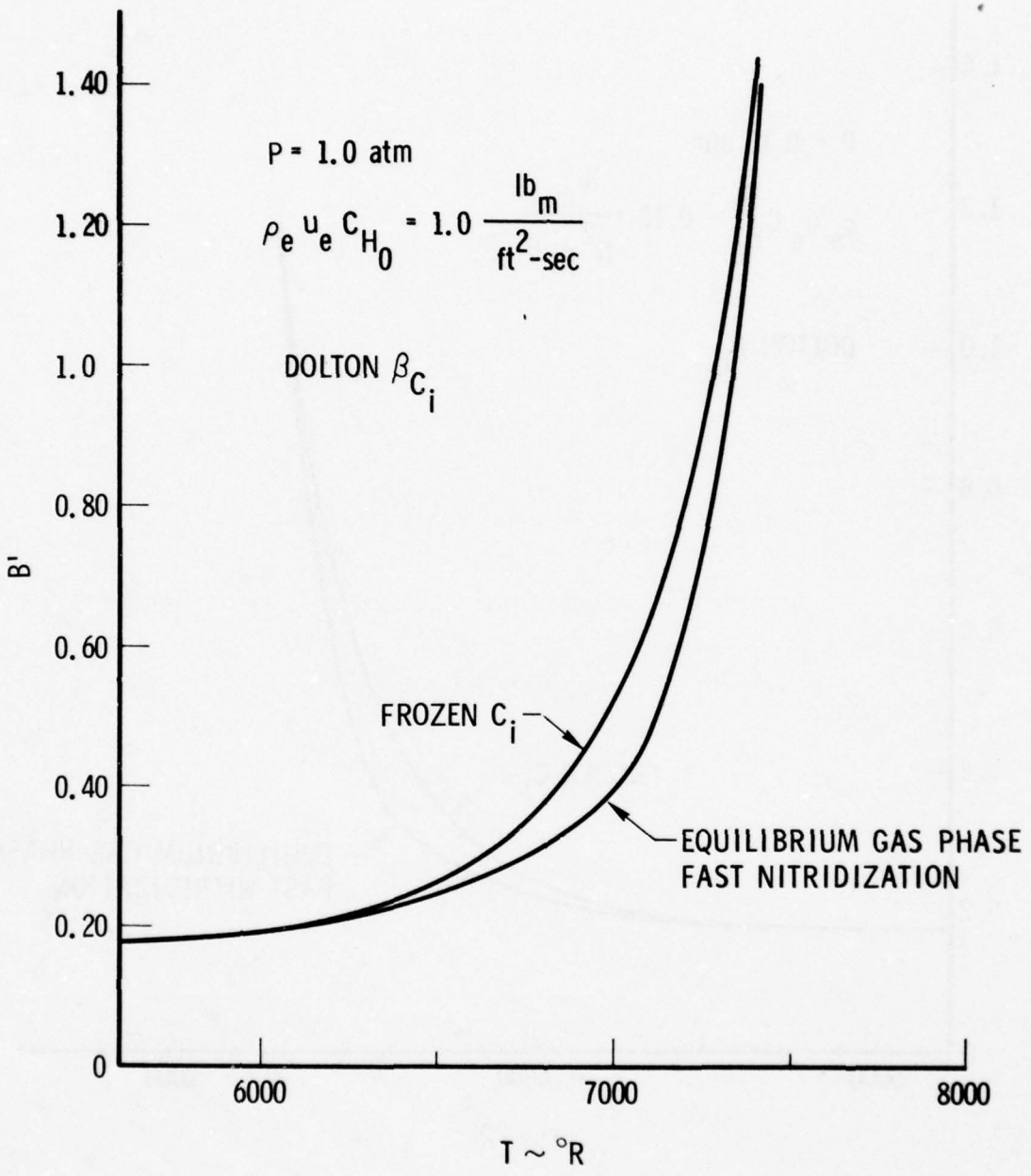


Fig. 12. Influence of Frozen Sublimation Species (P = 1.0 atm)

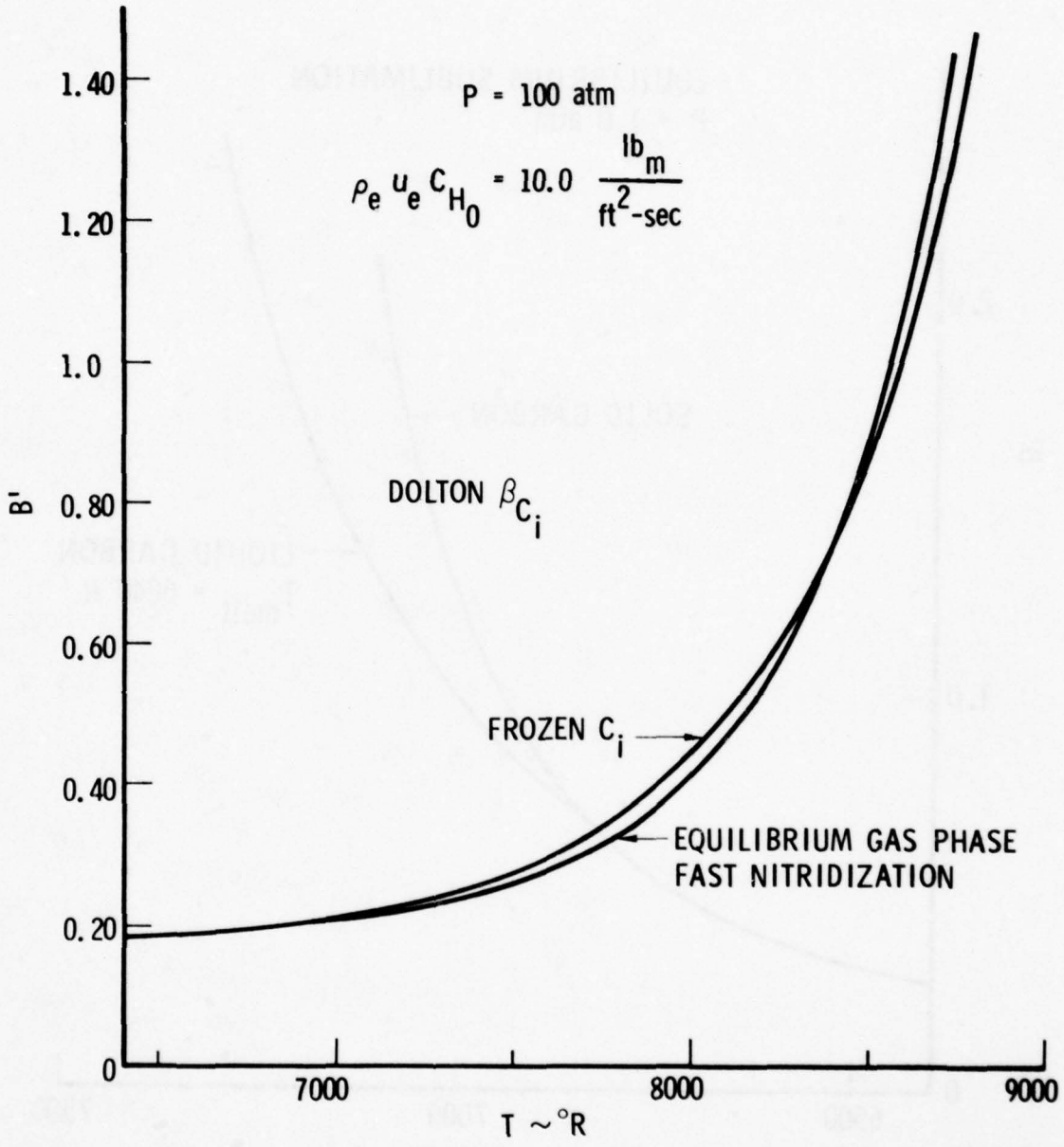


Fig. 13. Influence of Frozen Sublimation Species (P = 100 atm)

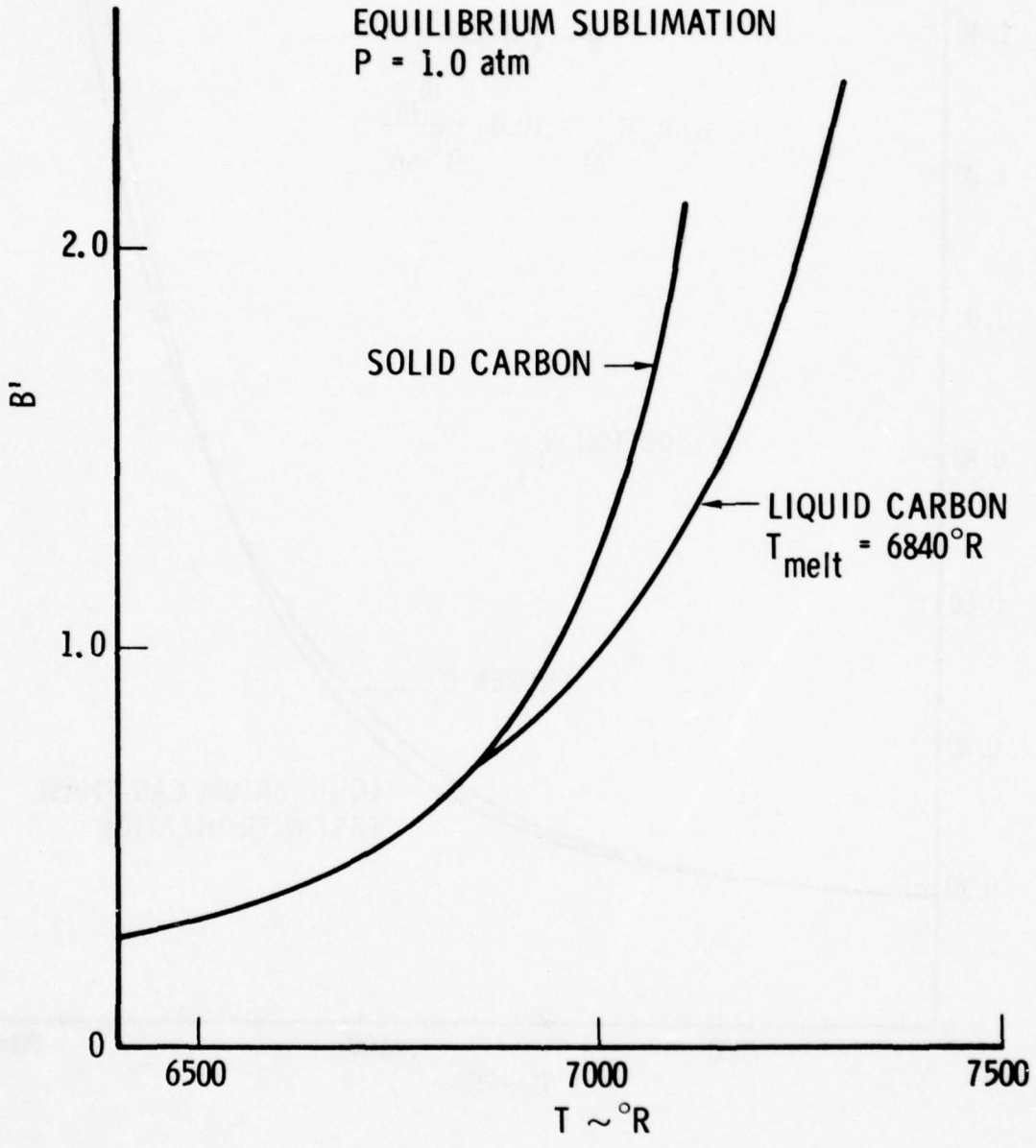


Fig. 14. Equilibrium Vaporization from a Carbon Melt Layer (P = 1.0 atm)

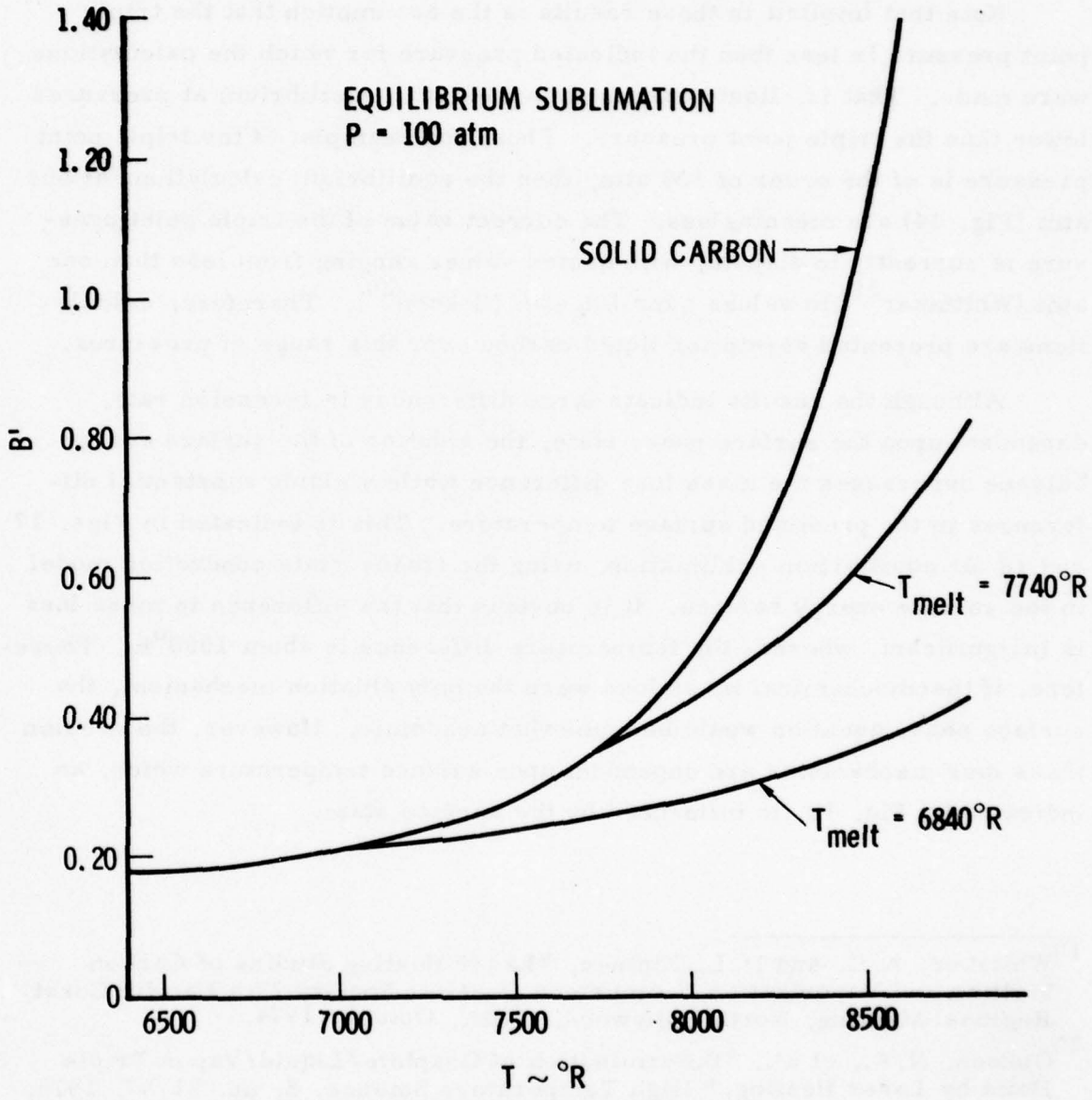


Fig. 15. Equilibrium Vaporization from a Carbon Melt Layer (P = 100 atm)

pressures and several melt temperatures. The nonequilibrium calculations show the same trend as seen in Fig. 16.

Note that implicit in these results is the assumption that the triple point pressure is less than the indicated pressure for which the calculations were made. That is, liquid carbon cannot exist in equilibrium at pressures lower than the triple point pressure. Thus, for example, if the triple point pressure is of the order of 100 atm, then the equilibrium calculations at one atm (Fig. 14) are meaningless. The correct value of the triple point pressure is currently in dispute, with quoted values ranging from less than one atm (Whittaker[19]) to values over 100 atm (Gokcen[20]). Therefore, calculations are presented herein for liquid carbon over this range of pressures.

Although the results indicate large differences in recession rate, dependent upon the surface phase state, the solution of the surface energy balance suppresses the mass loss difference while yielding substantial differences in the predicted surface temperature. This is indicated in Figs. 17 and 18 for equilibrium sublimation, using the steady-state conduction model in the surface energy balance. It is obvious that the difference in mass loss is insignificant, whereas the temperature difference is about 1000°R. Therefore, if thermochemical mass loss were the only ablation mechanism, the surface phase question would be somewhat academic. However, the erosion mass loss mechanisms are dependent upon surface temperature which, as indicated by Fig. 18, is influenced by the surface state.

---

[19] Whitaker, A.G. and P.L. Kintner, "Laser Heating Studies of Carbon Melting and Vaporization," American Ceramic Society 27th Pacific Coast Regional Meeting, North Hollywood, Calif., October 1974.

[20] Gokcen, N.A., et al., "Determination of Graphite/Liquid/Vapor Triple Point by Laser Heating," High Temperature Science, 8, pp. 81-97, 1976.

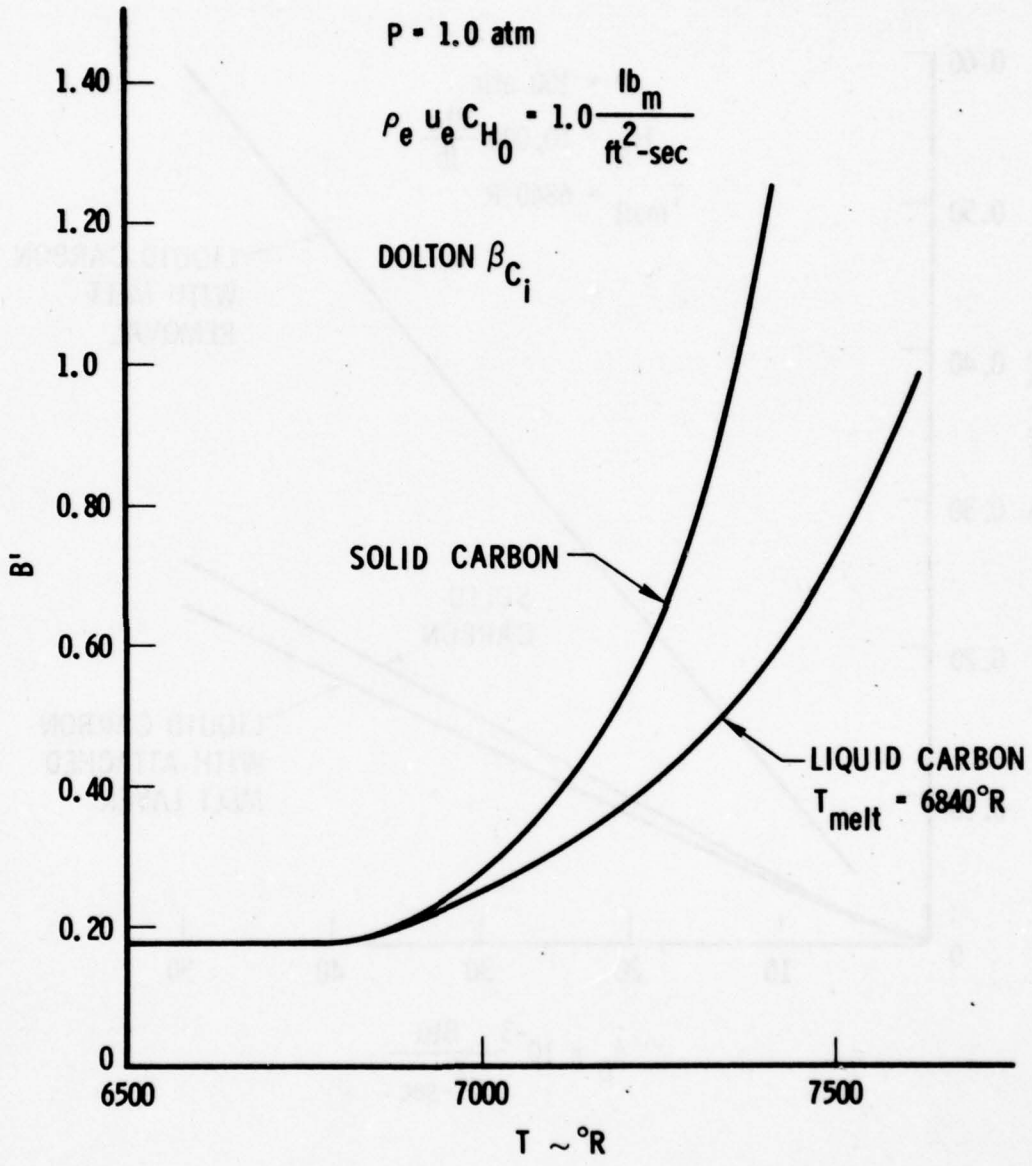


Fig. 16. Nonequilibrium Vaporization from a Carbon Melt Layer (P = 1.0 atm)

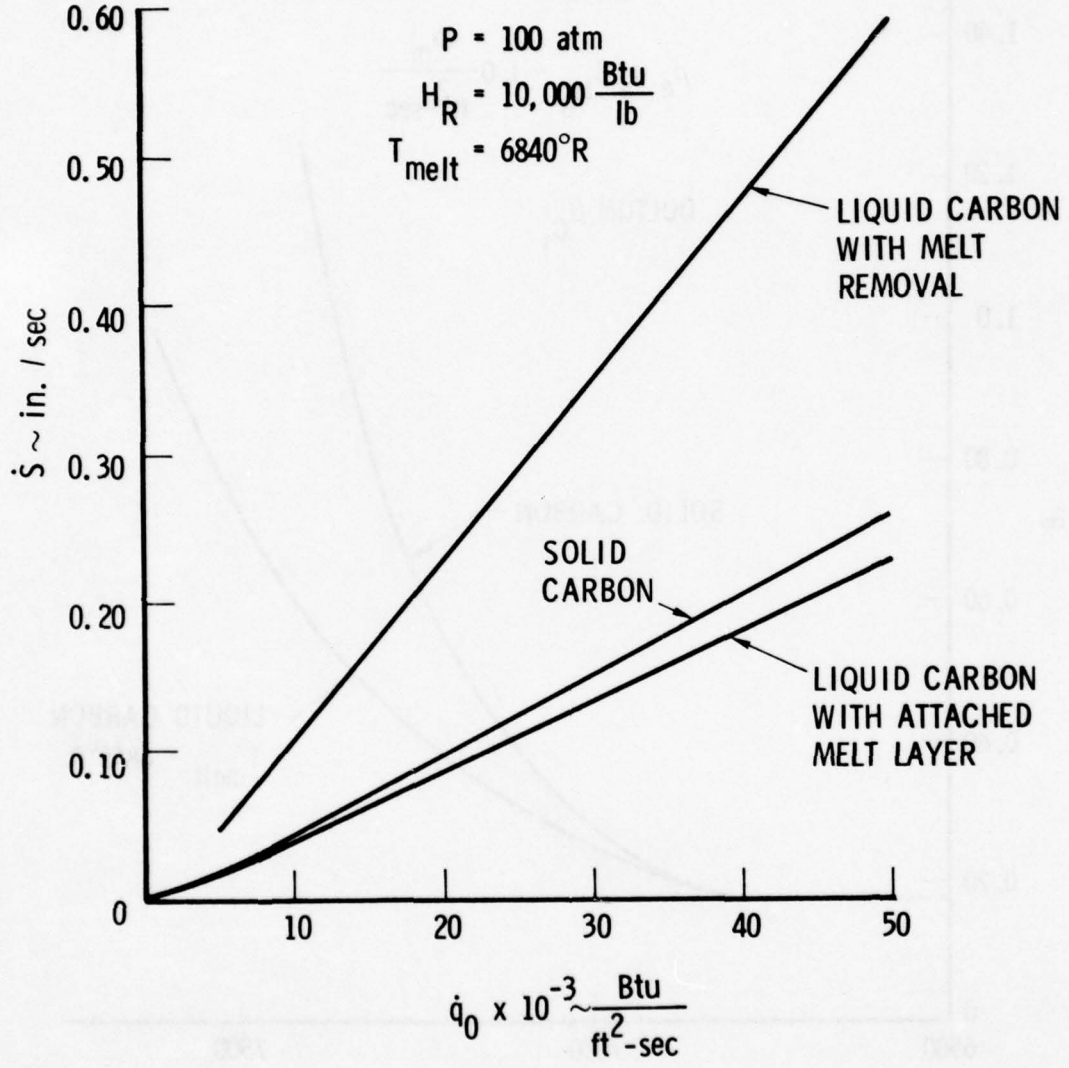


Fig. 17. Comparison of Solid and Liquid Carbon Ablation Models for Surface Recession

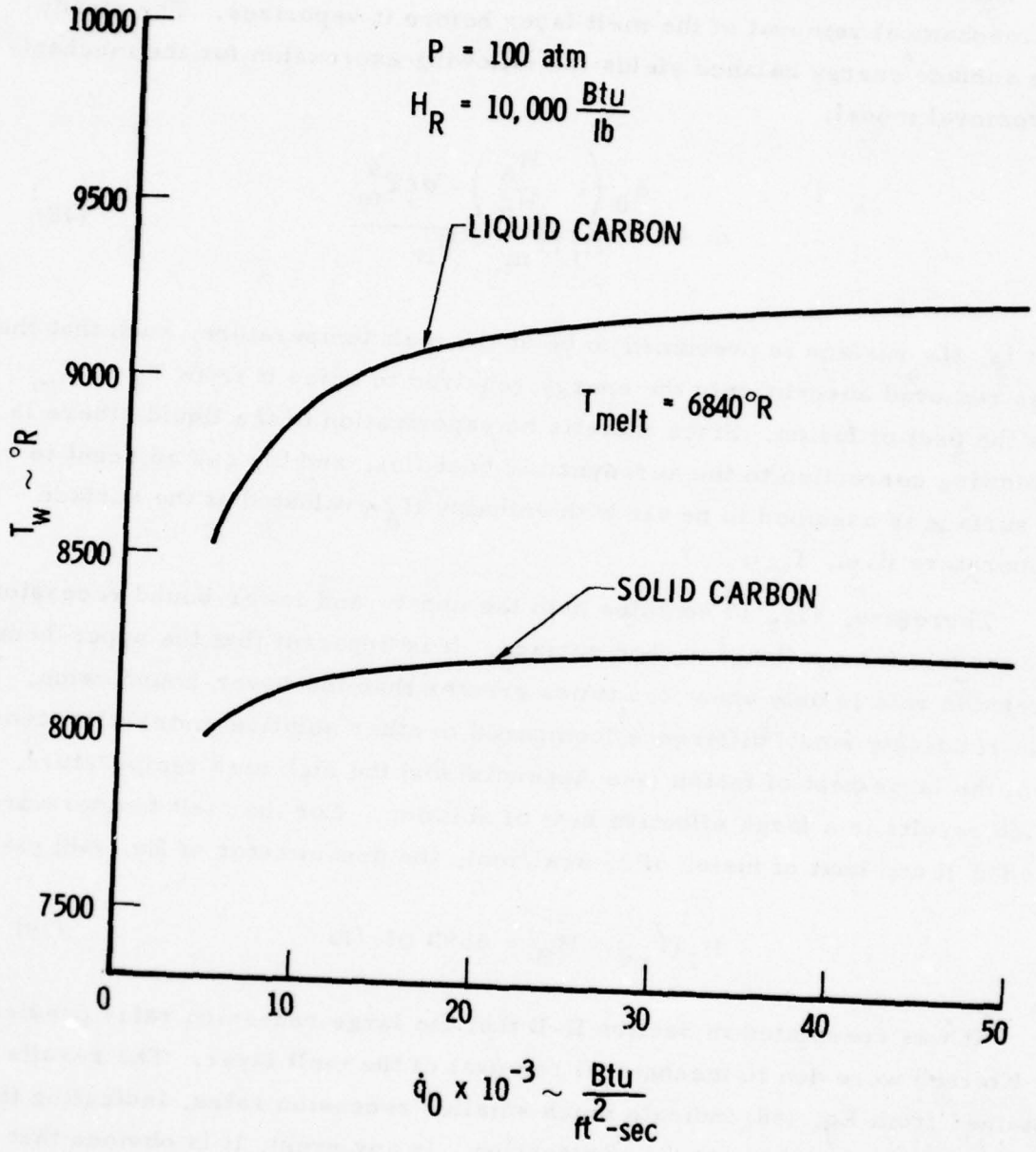


Fig. 18. Comparison of Solid and Liquid Carbon Ablation Models for Surface Temperature

Also shown in Fig. 17 is the upper-bound recession rate associated with mechanical removal of the melt layer before it vaporizes. The steady-state surface energy balance yields the following expression for the mechanical removal model:

$$\dot{m} = \frac{\dot{q}_0 \left(1 - \frac{H_A}{H_R}\right) - \sigma \epsilon T_m^4}{H_L(T_m) - H_B} \tag{48}$$

That is, the surface is presumed to be at the melt temperature, such that the mass removed absorbs only the energy required to raise it from T_B to T_m plus the heat of fusion. Since there is no vaporization of the liquid, there is no blowing correction to the aerodynamic heat flux, and the gas adjacent to the surface is assumed to be air with enthalpy H_A evaluated at the surface temperature (i.e., T_m).

Therefore, Fig. 17 contains both the upper- and lower-bound recession rate models from a liquid carbon surface. It is apparent that the upper-bound recession rate is only about 2.5 times greater than the lower-bound value. This relatively small difference (compared to other ablative materials) stems from the large heat of fusion (see Appendix) and the high melt temperature, which results in a large effective heat of ablation. For the melt temperature of $6840^{\circ}R$ and heat of fusion of 25 kcal/mol, the denominator of Eq. (48) yields

$$H_L(T_m) - H_B = 6590 \text{ Btu/lb} \tag{49}$$

It was speculated in Section II-D that the large recession rates predicted by Kratsch were due to mechanical removal of the melt layer. The results obtained from Eq. (48) indicate much smaller recession rates, indicating that mechanical removal is not the explanation. In any event, it is obvious that the present results are in total disagreement with those of Kratsch.

The steady-state melt layer thickness obtained from Eq. (44) is shown in Fig. 19 for two different values of recovery enthalpy. The liquid thermal diffusivity was assumed to be an order of magnitude smaller than the diffusivity of solid graphite[21]. Since the melt layer thickness is linear with the liquid diffusivity, the thickness for other values of σ_L may be obtained by scaling the values of Fig. 19.

The results indicate that the melt layer thickness for a flight environment will range from one mil to 10 mils depending upon the severity of the environment. Although these values are quite small relative to a typical nosetip radius, it cannot be stated that they are sufficiently small to resist flowing of the liquid carbon. Resolution of this question would require an analysis of the dynamics of the liquid layer and is beyond the scope of this report. The calculation for a low enthalpy flow (typical of a high-pressure arc jet) yields melt layer thicknesses less than half a mil. The greatly reduced thickness for the low enthalpy case is due to a much lower surface temperature ($\approx 7000^{\circ}R$) than that of Fig. 18. These small thicknesses may explain why molten carbon is not readily observable in high-pressure arc jet facilities.

F. STEADY-STATE CONDUCTION ASSUMPTION

As indicated in Subsection II-E, the use of the steady-state conduction assumption can lead to substantial errors in the predicted surface mass loss. In this subsection, calculations are presented for both the steady-state conduction model and the transient expression of Eq. (41). Nominal graphite properties were used, and the thermal diffusivity was taken as 0.0001 ft^2/sec. The surface energy balance was solved for several values of heat flux using the equilibrium sublimation assumption. The results are shown in Fig. 20, where it is apparent that the use of the steady-state conduction model overpredicts the recession by as much as a factor of two at early times. As

[21] White, H. M., "Estimation of Some Carbon Properties at the Triple Point," Report No. TOR-669(S6811-20)-12, The Aerospace Corporation, San Bernardino, Calif., June 1966.

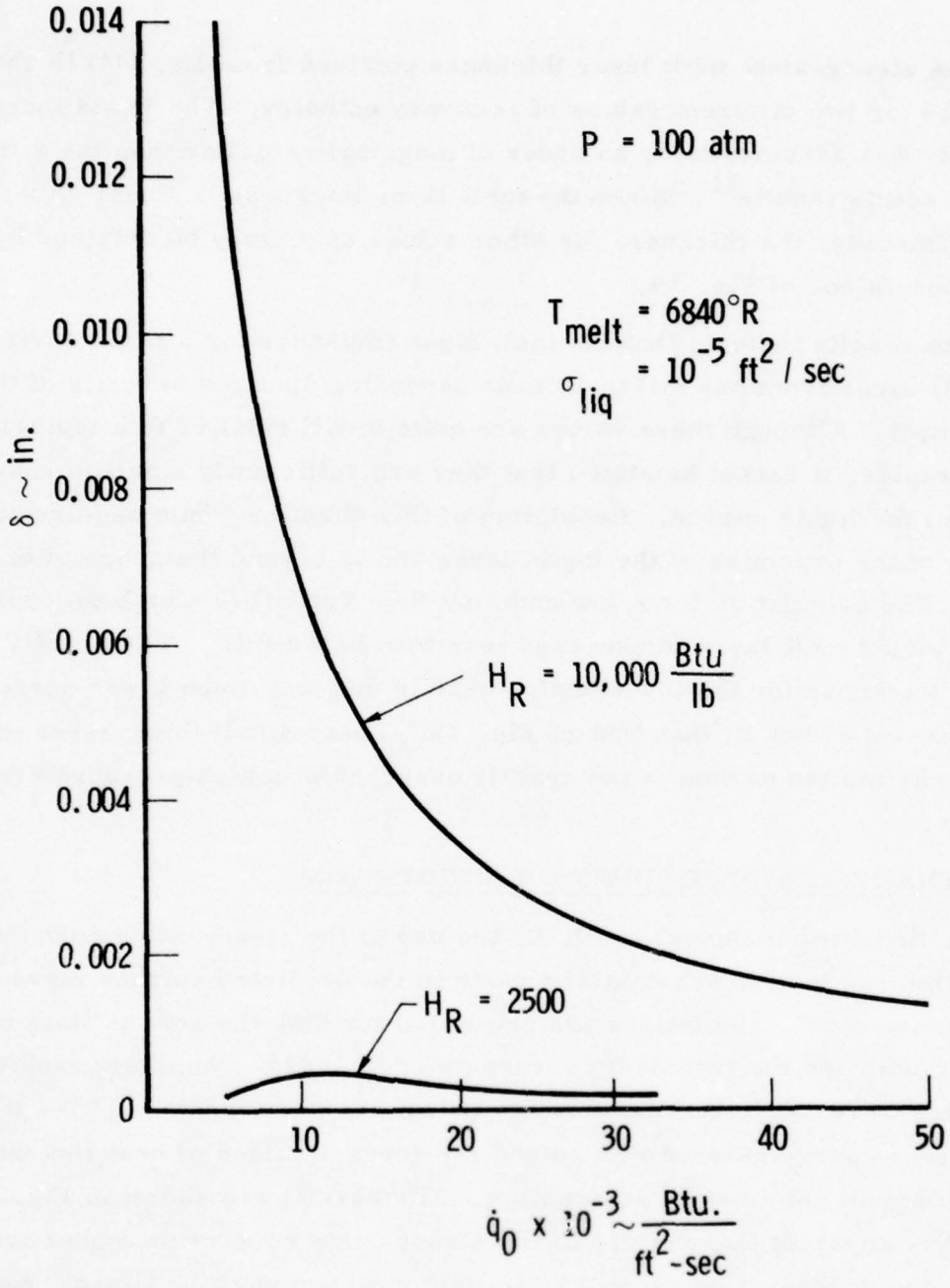


Fig. 19. Steady-State Melt Layer Thickness

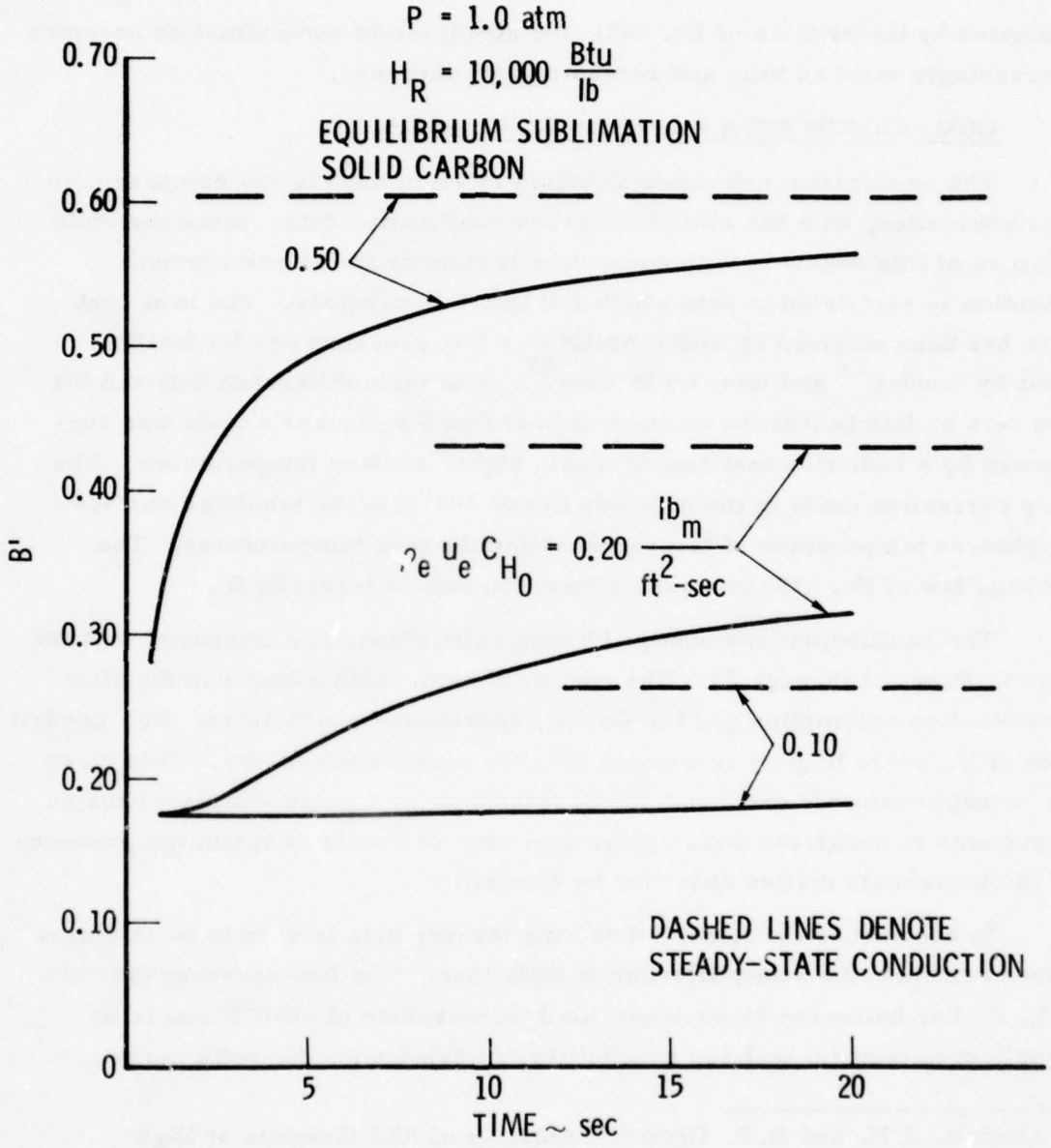


Fig. 20. Comparison of Steady-State and Transient Conduction Models for Surface Mass Transfer

indicated by the criteria of Eq. (42), the steady-state approximation becomes increasingly valid as time and recession rate increase.

G. COMPARISON WITH EXPERIMENTAL DATA

The equilibrium and nonequilibrium ablation models are compared, in this subsection, with the available carbon sublimation data. Since the main concern of this report is with convective heating in an air environment, attention is restricted to data which fall into this category. The best such data has been obtained at NASA-AMES in a low-pressure arc jet facility, first by Lundell[22] and later by Maurer[23]. The main difference between the two sets of data is that the convective heat flux for Maurer's tests was augmented by a radiative heat flux to obtain higher surface temperatures. The only correction made to the data was to add 100°K to the tabulated surface brightness temperature of Maurer to obtain the true temperatures. The blowing law of Eq. (13) was used to cast the data in terms of B'.

The equilibrium and nonequilibrium calculations are compared with the data in Figs. 21 through 23. The nonequilibrium calculations use the slow nitridization assumption and the Dolton vaporization coefficients. The Lundell data (Fig. 21) is in good agreement with the equilibrium theory. This close agreement obviously precludes the necessity of invoking mechanical erosion arguments to match the data. (This does not, of course, explain the presence of the particulate matter observed by Lundell.)

In contrast to the Lundell data, the Maurer data is seen to be in closer agreement with the nonequilibrium calculations. The low-pressure data of Fig. 23 lies below the lower bound melt temperature of 6840°R and is in excellent agreement with the nonequilibrium calculation for solid carbon.

---

[22] Lundell, J.H. and R.R. Dickey, "Ablation of ATJ Graphite at High Temperatures," AIAA Journal, 11(2), pp. 216-222, January 1973.

[23] Maurer, R.E., et al., "Graphite Sublimation Under Low and High Convective Mass Transfer Environments," ASME Paper 76-ENAS-68, July 1976.

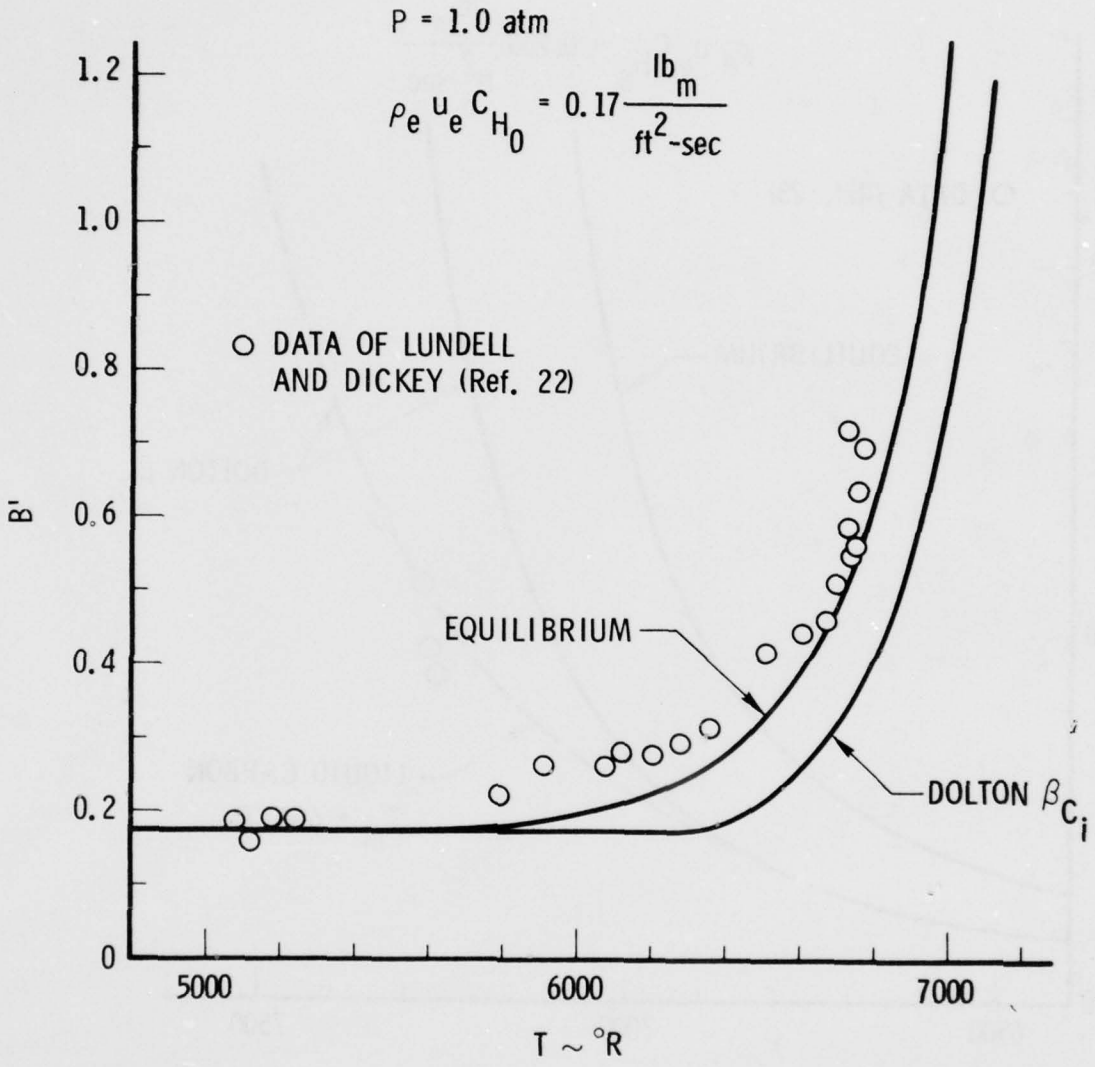


Fig. 21. Comparison of Equilibrium and Nonequilibrium Ablation Models with Lundell Data (P = 1.0 atm)

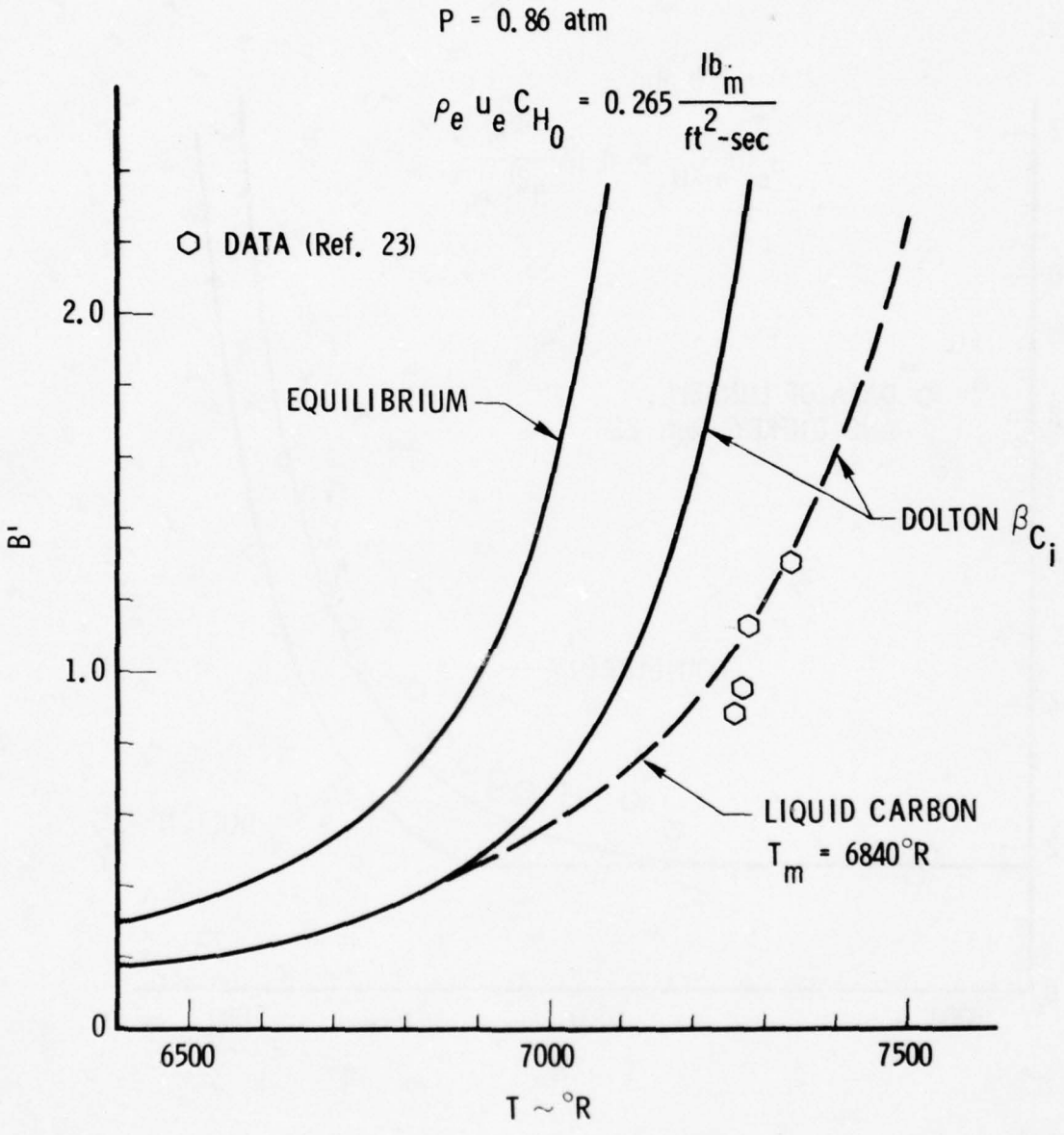


Fig. 22. Comparison of Equilibrium and Nonequilibrium Ablation Models with Maurer Data (P = 0.86 atm)

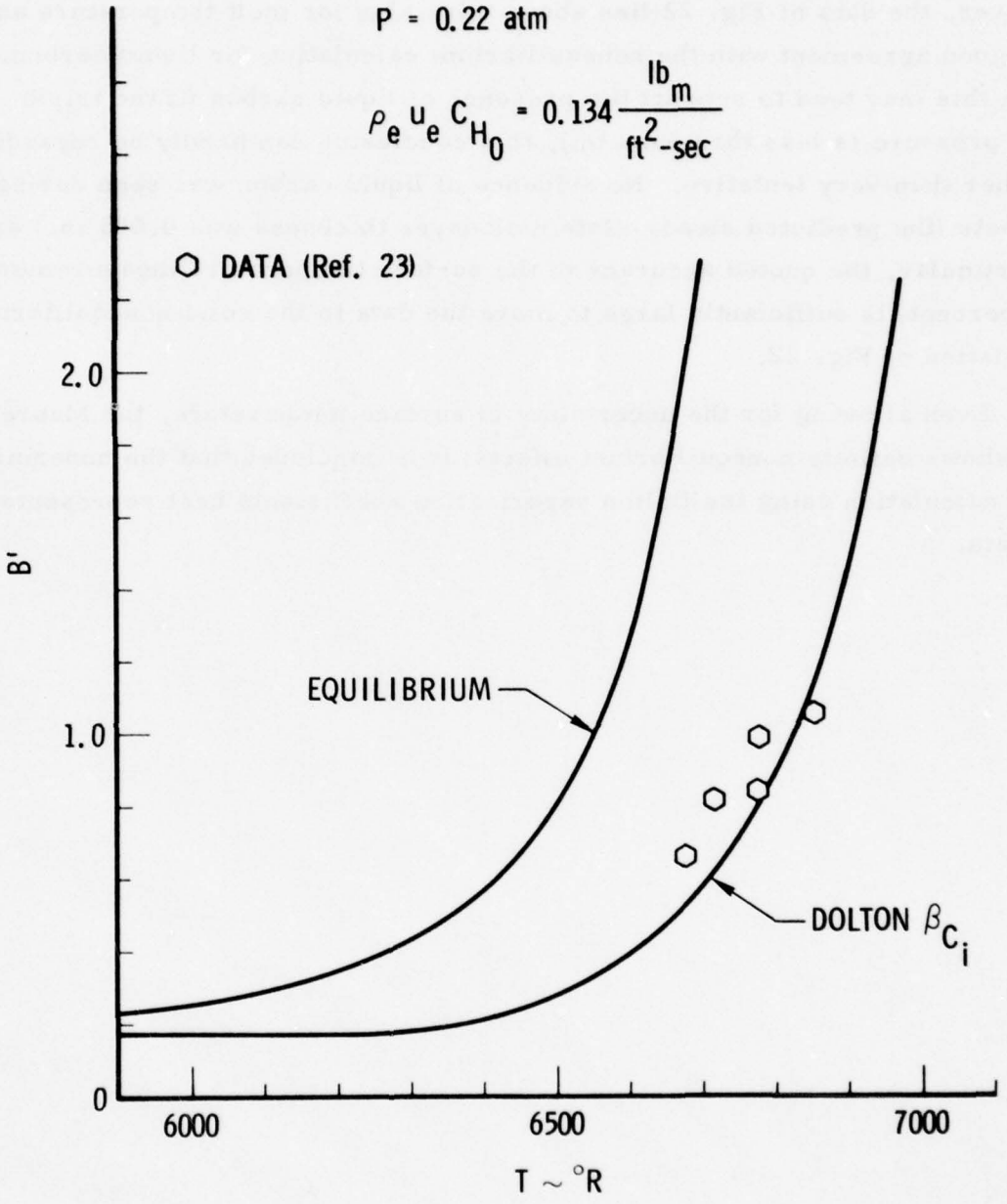


Fig. 23. Comparison of Equilibrium and Nonequilibrium Ablation Models with Maurer Data (P = 0.22 atm)

However, the data of Fig. 22 lies above this value for melt temperature and is in good agreement with the nonequilibrium calculation for liquid carbon. While this may tend to support the presence of liquid carbon (if the triple point pressure is less than one atm), this conclusion can hardly be regarded as other than very tentative. No evidence of liquid carbon was seen during the tests (the predicted steady-state melt layer thickness was 0.003 in.) and, in particular, the quoted accuracy of the surface temperature measurements (± 2 percent) is sufficiently large to move the data to the solid nonequilibrium calculation of Fig. 22.

Even allowing for the uncertainty in surface temperature, the Maurer data shows definite nonequilibrium effects; it is concluded that the nonequilibrium calculation using the Dolton vaporization coefficients best represents the data.

IV. SUMMARY AND CONCLUSIONS

An examination of the nonequilibrium carbon ablation process has been presented. The study has focused on the shortcomings of the available analyses and has undertaken a systematic examination of the assumptions that are usually invoked in the nonequilibrium model for carbon ablation. The major areas of investigation included the influence of the assumed chemical state (i.e., frozen or equilibrium reactions), ablation from a molten carbon surface, and the computational considerations associated with solving the system of equations.

The assumptions of fast and slow heterogeneous nitridization reactions were examined in conjunction with an equilibrium gas phase. The results indicated significant recession rate differences only for extreme departures from equilibrium. It was concluded that, for the nominal range of pressure and heat flux for ground test and flight environments, the differences are small (on the order of 10 percent). The assumption that the carbon sublimation species are frozen in the gas phase was also examined and found to exert no significant influence on the recession rate.

Although the various reaction rate assumptions were found to exert only small influences on the recession rate, the only self-consistent model was found to be the slow nitridization assumption with an equilibrium gas phase. Comparisons of the slow nitridization model with experimental data show reasonable agreement (using Dolton vaporization coefficients), and this model is recommended for adoption.

The sublimation from a liquid carbon surface was handled by assuming that the melt layer was sufficiently thin to adhere to the surface without mechanical removal. The liquid carbon assumption was found to result in a substantial reduction of the predicted B', as compared to the value obtained for vaporization from a solid surface. Application of the carbon melt

layer calculation to flight environments yielded slightly lower recession rates than the solid carbon assumption but with an increase in surface temperature of about 1000°R. It is hoped that these results will provide some impetus for the experimental investigation of the liquid layer hypothesis in ground test arc jet facilities.

A unified analysis of the nonequilibrium carbon ablation process has been presented by treating the oxidation and sublimation regimes simultaneously. A computationally efficient solution procedure, requiring only a single iteration loop, is utilized to solve the system of equations. Convergence of the iteration scheme is sufficiently fast to utilize the method as a subroutine package for inclusion into thermodynamic material response codes.

Finally, some comments concerning recommendations for future ablation tests are in order. The analysis of this report has treated the vaporization coefficients as known quantities. The results of this investigation indicate that the uncertainties in the vaporization coefficients exert substantially more influence on the ablation predictions than do the uncertainties in the gas/solid reaction rates. In order to experimentally investigate the vaporization process in the absence of chemical reactions, it is recommended that a series of arc jet ablation tests be carried out in an inert atmosphere. Both ATJ-S and the current carbon-carbon composite materials should be tested. In addition, since no carbon-carbon ablation data exists in the sublimation regime, arc jet tests are also required for this material in air.

Further areas of investigation should include experiments to determine the C_2N heat of formation and reaction rates for heterogeneous carbon-nitrogen reactions, for both graphite and carbon-carbon.

REFERENCES

1. Crowell, P.G., "Analytic Solutions for Carbon Sublimation in Atmospheres of Elemental Carbon, Hydrogen, Nitrogen and Oxygen," Report No. TR-0078(3550-15)-2, The Aerospace Corporation, El Segundo, Calif., December 1977.

2. Maurer, R.E., "An Evaluation of Some Uncertainties in Carbon Sublimation Kinetics," Aerotherm TM-73-27, January 1973.

3. Kratsch, K.M., "Graphite Fusion and Vaporization," ASME/AIAA 10th Structures, Structural Dynamics and Materials Conference, April 1969.

4. Dolton, T.A., R.E. Maurer, and H.E. Goldstein, "Thermodynamic Performance of Carbon in Hyperthermal Environments," AIAA 3rd Thermophysics Conference, Paper No. 68-754, June 1968.

5. Baker, R.L., "Graphite Sublimation Chemistry Nonequilibrium Effects," AIAA Journal, 15(10), October 1977.

6. Ziering, M.B. and V. DiCristina, "Thermomechanical Erosion of Ablative Plastic Composites," AIAA 7th Thermophysics Conference, April 1972, Paper No. 72-299.

7. JANNAF Thermochemical Tables, National Bureau of Standards, NBS-37, June 1971.

8. Kennard, E.H., "Kinetic Theory of Gases," McGraw-Hill Book Co., Inc., New York, 1938.

9. Goldstein, H.W., "The Reaction of Active Nitrogen with Graphite," Journal of Physical Chemistry, 68(1), January 1964.

10. Dorrance, W.H., "Viscous Hypersonic Flow," McGraw-Hill Book Co., Inc., New York, 1962.

11. Carslaw, H.S. and J.C. Jaeger, Conduction of Heat in Solids, Oxford University Press, 1959, p. 388.

12. Hansen, C.F. and W.E. Pearson, "A Quantum Model for Bending Vibrations and Thermodynamic Properties of C_3," Canadian Journal of Physics, 51, 1973.

13. Pearson, W.E. and W.C. Davy, "New Thermodynamic Functions for the C_3 Molecule," AIAA Journal, 11(8), August 1973.

REFERENCES (Continued)

14. Strauss, H. L. and E. Thiele, "Thermodynamics of C_3 General Methods for Nonrigid Molecules at High Temperature," Journal of Chemical Physics, 46(7), April 1967.

15. Wachi, F.M. and D.E. Gilmartin, "Heat of Formation and Entropy of C_3 Molecule," Report No. TR-0172(2250-40)-7, The Aerospace Corporation, El Segundo, Calif., May 1972.

16. Meyer, J.A. and D.W. Setser, "Chemiluminescence from the Reaction of Oxygen Atoms with Dicyanoacetylene," Journal of Physical Chemistry, 74, 1970, p. 3452.

17. Hirth, J.P., "Evaporation and Sublimation Mechanisms," The Characterization of High Temperature Vapors, J. L. Margrave (ed.), John Wiley & Sons, Inc., New York, 1967.

18. Bernstein, H. and J.R. Baron, "Stability Characterization of Refractory Materials Under High Velocity Atmospheric Flight Conditions, Part IV, Volume II, Calculation of the General Surface Reaction Problem," AFML TR-69-84, December 1969.

19. Whitaker, A.G. and P.L. Kintner, "Laser Heating Studies of Carbon Melting and Vaporization," American Ceramic Society 27th Pacific Coast Regional Meeting, North Hollywood, Calif., October 1974.

20. Gokcen, N.A., et al., "Determination of Graphite/Liquid/Vapor Triple Point by Laser Heating," High Temperature Science, 8, pp. 81-97, 1976.

21. White, H.M., "Estimation of Some Carbon Properties at the Triple Point," Report No. TOR-669(S6811-20)-12, The Aerospace Corporation, San Bernardino, Calif., June 1966.

22. Lundell, J.H. and R.R. Dickey, "Ablation of ATJ Graphite at High Temperatures," AIAA Journal, 11(2), pp. 216-222, January 1973.

23. Maurer, R.E., et al., "Graphite Sublimation Under Low and High Convective Mass Transfer Environments," ASME Paper 76-ENAS-68, July 1976.

24. Powars, C.A. and R.M. Kendall, "User's Manual--Aerotherm Chemical Equilibrium (ACE) Computer Program," Aerotherm Corporation, May 1969.

APPENDIX A

VAPOR PRESSURE OF CARBON SUBLIMATION SPECIES

As discussed in the main text (Section II), the vapor pressure of each gaseous carbon species is assumed to be a known function of temperature. These vapor pressures are presented in this Appendix for vaporization from both solid and liquid carbon surfaces. The solid vaporization case is considered first.

A. VAPORIZATION FROM SOLID CARBON

The gaseous carbon species in equilibrium with the solid carbon surface are denoted by C_i. The vaporization reaction is given as

$$i\, C_{solid} \longrightarrow C_i \tag{A-1}$$

For this reaction, the third law gives

$$\ell n\, P_{C_i} = \frac{-E_0(C_i)}{RT} - \left(\frac{F^0 - H_0^0}{RT}\right)_{C_i} + i\left(\frac{F^0 - H_0^0}{RT}\right)_{solid} \tag{A-2}$$

where $H_0^0(C_i)$ is the heat of formation of C_i at $0^\circ K$, and the heat of formation of solid carbon has been set equal to zero by convention.

The free-energy function and partition function for the gaseous species are related as follows:

$$\left(\frac{F^0 - H_0^0}{RT}\right)_{C_i} = -\ell n\, Q_p(C_i) \tag{A-3}$$

The free-energy function is related to the specific heat by

$$\frac{F^0 - H^0_{298}}{T} = \frac{1}{T}\int_{298}^{T} C_p dT - \int_{298}^{T} \frac{C_p}{T} dT - S^0_{298} \qquad (A-4)$$

Note that the JANNAF[7] thermochemical data uses a base temperature of 298°K. The free-energy functions at 0°K and 298°K are related by

$$\frac{F^0 - H^0_0}{T} = \frac{F^0 - H^0_{298}}{T} - \frac{H^0_0 - H^0_{298}}{T} \qquad (A-5)$$

The free-energy function referenced to 298°K and the difference in enthalpies between 0°K and 298°K are both tabulated in JANNAF.

For solid carbon, the JANNAF data yields

$$\frac{F^0 - H^0_0}{T} = \frac{F^0 - H^0_{298}}{T} + \frac{252}{T} \qquad (A-6)$$

The curve fits for specific heat in the ACE code were used to evaluate the free-energy function for solid carbon by using Eq. (A-4). The final result is

$$\frac{F^0 - H^0_{298}}{T} = A(1 - \ell nT) - \frac{1}{2}BT - \frac{C}{2T^2} - \frac{D}{T} + E \qquad (A-7)$$

$T \leq 3000°K$:

$A = 5.861$

$B = 0.954 \times 10^{-4}$

$C = -0.7666 \times 10^{6}$

$D = 4323.3$

$E = 35.235$

$T \geq 3000^{\circ}K$:

$$A = 4.85$$
$$B = 0.2916 \times 10^{-3}$$
$$C = 0.3072 \times 10^{7}$$
$$D = 893.7$$
$$E = 27.516$$

where all temperatures are in $^{\circ}K$, and the units of the free-energy functions are cal/mol-$^{\circ}K$.

The use of Eqs. (A-6) and (A-7) in Eq. (A-2) provides all the necessary information about the solid phase.

The partition functions were used to obtain the free-energy functions for the gaseous carbon species (with the exception of C_3). The C_3 free energy function was obtained from the curve fit by Pearson[13].

The enthalpy of solid carbon is required in the surface energy balance and is given by

$$H^0(S) = AT + \frac{1}{2} BT^2 - \frac{C}{T} + 252 - D \qquad \text{cal/mol} \qquad (A-8)$$

where (S) denotes solid properties.

B. VAPORIZATION FROM LIQUID CARBON

For vaporization from a liquid carbon surface, the third law yields

$$\ell n\, P_{C_i} = \frac{-\Delta H^0}{RT} - \left(\frac{F^0 - H_0^0}{RT}\right)_{C_i} + i\left(\frac{F^0 - H_{T_m}^0}{RT}\right)_{\text{liquid}}$$

$$\Delta H^0 \equiv H_0^0(C_i) - i\, H_{T_m}^0\,(L) \qquad (A-9)$$

where (L) denotes liquid properties, and T_m denotes a quantity evaluated at the melt temperature.

The liquid carbon free energy function is given by

$$\left(\frac{F^0 - H^0_{T_m}}{T}\right)_{liquid} = \frac{1}{T}\int_{T_m}^{T} C_p(L)dT - \int_{T_m}^{T}\frac{C_p(L)}{T}dT - S^0_{T_m}(L) \qquad (A-10)$$

The entropy and enthalpy of the liquid, at the melt temperature, are related to the corresponding solid values through the heat of fusion.

$$H^0_{T_m}(L) = H^0_{T_m}(S) + \Delta H^0_F$$

$$S^0_{T_m}(L) = S^0_{T_m}(S) + \frac{\Delta H^0_F}{T_m} \qquad (A-11)$$

The enthalpy and entropy of the solid, at the melt temperature, are obtained from the JANNAF data.

The additional data required to evaluate these expressions is the melt temperature, the specific heat of liquid carbon, and the heat of fusion at the melt temperature. The following values were obtained from White[21]:

$$\Delta H_F = 25 \text{ Kcal/mol}$$

$$C_p(L) = 7.44 \text{ cal/mol-}^\circ\text{K} \qquad (A-12)$$

For a constant value of the liquid carbon specific heat, the free-energy function of Eq. (A-10) becomes

$$\left(\frac{F^0 - H^0_{T_m}}{T}\right)_{liquid} = C_p(L)\left[1 - \frac{T_m}{T} + \ell n\,\frac{T_m}{T}\right] - S^0_{T_m}(L) \qquad (A-13)$$

The lower-bound melt temperature of 3800°K, obtained by Whittaker[19], was used in most of the calculations. The JANNAF values for solid carbon, at this temperature, are given as

$$T_m = 3800^{\circ}K$$

$$H^0_{T_m}(S) = 19559 \text{ cal/mol}$$

$$S^0_{T_m}(S) = 13.575 \text{ cal/mol-}^{\circ}K \qquad \text{(A-14)}$$

The enthalpy of the liquid carbon surface is required to solve the surface energy balance and is given as

$$H^0(L) = H^0_{T_m}(S) + \Delta H^0_F + \int_{T_m}^{T} C_p(L)\, dT \qquad \text{(A-15)}$$

All the calculations of this report used a constant value of $C_p(L)$, for which the integral of Eq. (A-15) is easily evaluated.

Finally, it is instructive to examine the ratio of liquid to solid vapor pressures for temperatures greater than the melt temperature. The third law relationships of Eqs. (A-1) and (A-9) are combined to yield

$$\ell n \frac{P_{C_i}(L)}{P_{C_i}(S)} = i\left[\frac{F^0(L)}{RT} - \frac{F^0(S)}{RT}\right] \qquad \text{(A-16)}$$

Substitution of the free-energy functions into this expression yields

$$\ell n \frac{P_{C_i}(L)}{P_{C_i}(S)} = \frac{i}{R}\left\{\left(\frac{1}{T} - \frac{1}{T_m}\right)\Delta H^0_F + \frac{1}{T}\int_{T_m}^{T} [C_p(L) - C_p(S)]\, dT - \int_{T_m}^{T} \frac{C_p(L) - C_p(S)}{T}\, dT\right\} \qquad \text{(A-17)}$$

It is apparent that the second integral is larger in magnitude than the first integral provided that the liquid specific heat exceeds the solid specific heat. This is clearly the case for the value of Eq. (A-12) (as compared with the tabulated JANNAF values). Thus, for $T > T_m$ it is obvious that the right-hand side of Eq. (A-17) is negative. Therefore, the vapor pressure of carbon species C_i, in equilibrium with a liquid carbon surface, is less than the vapor pressure of the same species in equilibrium with a solid carbon surface at a temperature greater than the melt temperature. That is

$$P_{C_i}(L) \leq P_{C_i}(S) \qquad \text{(A-18)}$$

APPENDIX B

SELECTION OF CHEMICAL SPECIES

At the suggestion of the review committee, additional discussion and justification for the choice of included species is provided in this appendix.

The choice of allowable species was constrained by accuracy and computational considerations. Thus, all of the dominant species identified by previous investigators were automatically included. Only two minor species were included (atomic oxygen and nitrogen) because they are potentially important with respect to the heterogeneous oxidation and nitridization reactions, and their inclusion does not impact the solution procedure.

The inclusion of nitrogen-oxygen species into the formulation introduces additional iteration loops into the solution procedure, is computationally expensive, and is not warranted in terms of accuracy. At high temperatures, the nitrogen must compete with the carbon for the available oxygen, and since oxygen reacts far more readily with carbon, there is very little excess oxygen available for the formation of nitrogen-oxygen compounds. At low temperatures, where excess oxygen is available, the relevant equilibrium constants are so small that nitrogen-oxygen compounds exist only as trace species. These intuitive considerations were checked by running some exact equilibrium cases with the ACE[24] code over the range of pressures and temperatures of interest. The results verify that the nitrogen-oxygen compounds are insignificant. Thus, none of these species are included in the formulation.

The ACE results also indicate that the only significant carbon-oxygen species are CO and CO_2 and these are the only such species included.

---

[24] Powars, C.A. and R.M. Kendall, "User's Manual--Aerotherm Chemical Equilibrium (ACE) Computer Program," Aerotherm Corporation, May 1969.

The only carbon sublimation species included were those for which reliable spectroscopic data exists (i.e., C_1-C_5). Although some investigations have included carbon species up to C_{31}, their properties were obtained from theoretical models utilizing assumption of unknown accuracy. Although the inclusion of the higher order carbon species does not impose any additional computational difficulty, it was felt that the uncertainty associated with their thermochemical properties data justified their deletion.

NOMENCLATURE

B'	mass transfer parameter [defined in Eq. (3)]
H_B	enthalpy of solid carbon evaluated at some specified bulk temperature
$H_L(T)$	enthalpy of liquid carbon at temperature, T
H_R	recovery enthalpy
H_S	enthalpy of carbon surface phase (either liquid or solid)
H_w	enthalpy of gas mixture adjacent to surface
K_P	pressure equilibrium constant
K_i	mass fraction of species i
$\tilde{K}_i$	mass fraction of element i
M	molecular weight of gas mixture
M_I	molecular weight of inert species
M_i	molecular weight of species i
M_{C_i}	molecular weight of carbon sublimation species C_i
$\dot{m}$	total carbon mass loss
$\dot{m}_i$	mass loss due to heterogeneous reaction of carbon with species i
P	surface pressure
P_i	partial pressure of species i
$P^v_{C_i}$	equilibrium vapor pressure of carbon sublimation species C_i
$\dot{q}_o$	cold wall, nonblowing heat flux
R	universal gas constant
$\dot{S}$	surface recession rate
T	temperature
t	time

β_{C_i}	vaporization coefficients for carbon sublimation species
δ	carbon melt layer thickness
$\rho_e u_e C_H$	cold wall, blowing heat flux parameter = $\dot{q}/H_R$
$\rho_e u_e C_{H_0}$	cold wall, nonblowing heat flux parameter = $\dot{q}_o/H_R$
σ	thermal diffusivity

Subscripts

e	boundary layer edge values
L	liquid carbon
w	wall (surface) values

Superscripts

*	denotes a heterogeneous carbon-nitrogen reaction
~	denotes an element